December 2020

Sequence Components Based Detection and Classification of Faults in an Islanded Distribution System with 100% Inverter Based Resources

Ahmad Nasir Nadeeb
Clemson University, nasirnadib@yahoo.com

SEQUENCE COMPONENTS BASED DETECTION AND CLASSIFICATION OF FAULTS IN AN ISLANDED DISTRIBUTION SYSTEM WITH 100% INVERTER BASED RESOURCES

A Thesis
Presented to
the Graduate School of
Clemson University

In Partial Fulfillment
of the Requirements for the Degree
Master of Science
Electrical Engineering

---

by
Ahmad Nasir Nadeeb
December 2020

Accepted by:
Dr. Sukumar Brahma, Committee Chair
Dr. E. Randolph Collins
Dr. Ramtin Hadidi

Abstract

Traditional distribution systems, which are single-sourced and radial, are mostly protected by fuses, reclosers, and overcurrent relays. Due to the penetration of distributed energy resources, the topology changes to multi-sourced. Fuses and reclosers fail to coordinate for bidirectional fault currents flowing in such a system, jeopardizing the selectivity of protection. When these resources are Inverter Based Resources (IBRs), even detection and classification of faults becomes an issue due to lack of negative and zero sequence currents and severely restricted positive sequence fault currents contributed by IBRs. This issue is most prominent in an islanded distribution system fed completely by IBRs.

Recognizing that even in such an island where sequence currents are not generated by IBRs, sequence *voltages* will always be created by the physics of the fault and hence will be available at the IBR terminals, this thesis proposes to use these sequence voltages for detection and classification of faults locally at the IBR terminal. It also explores the possibility of using machine learning to approximately locate the faulted section based on the signatures provided by the local sequence voltages at the inverter terminal. IEEE 13-bus distribution feeder is modeled as an island in the time domain, fed by one grid forming and three grid following inverters to analyze the properties of such an unbalanced island in normal and faulted conditions. Based on the simulation results, insights are developed, and methodologies are formed and tested.

Acknowledgements

I would like to express my deepest gratitude to my advisor Dr. Sukumar Brahma during writing my research at Clemson University. It is a great honor to work with him. I am thankful for his help, patience, and providing his knowledge throughout studying my masters. This thesis would not have been accomplished without his constructive feedbacks, valuable comments, and his efforts.

I would like to also thank Dr. E. Randolph Collins for his support during studying for my graduate degree and his time, which he spared for me for talking and chatting. Thanks to Dr. Ramtin Hadidi, I learned a lot from him during writing this thesis and the two courses that I took with him.

Finally, I would like to thank my fiance Sonia for her patience and support during two years of studying for my master's.

Contents

List of Figures

List of Tables

Chapter 1

Introduction

One of the features of the smart grid is integrating decentralized renewable energy sources (e.g., solar panels and small wind turbines) into the electric power distribution systems. The penetration of renewable energy has increased worldwide over the last decade due to its decreasing cost and also due to the fact that traditional fossil fuel power plants change the earth climate by producing more greenhouse gases. In the U.S., 29 states have set their Renewable Portfolio Standards(RPS) in which there is a requirement for producing power from renewable sources in the future. Washington DC and New York have increased their renewable requirement in their RPS to 100% by 2032 and 2040, respectively. States like California, Hawaii, New Mexico, Virginia, Washington have set the requirement to produce all their energy from renewable sources by 2045 [1, 2].

Renewable energy sources use inverter to change their DC voltage or variable AC voltage to AC voltage in order to connect to the electric power distribution system. These sources are also called IBR (Inverter Based Resources). IBRs connects to the electric power distribution systems in either grid connected mode or islanded mode.

Grid connected distribution has both IBR and traditional power plants for supply of power. However, in islanded mode, the power is supplied totally by IBRs. The literature focuses more on protection in grid-connected mode rather than islanded distribution system. As distribution systems with 100% IBR are becoming a target in the U.S. and worldwide, this thesis will discuss the protection of islanded distribution system fed by 100% IBR, a unique and most difficult topology for protection that has gathered little attention.

Protection of the islanded distribution system fed 100% by IBRs, is a challenge for the utilities and power system engineers. One of the reasons IBR poses problems for the protection of distribution systems is that commercial inverters used in utilizing renewable energy limit the current close to the rated current(1.1pu) during faults to protect its component devices [3]. Thus, the islanded distribution system has substantially lower fault currents not amenable to traditional overcurrent devices. The commercial inverters also block the zero, and negative sequence currents [4]. This creates hindrance in sequence current based fault detection and classification, as well as coordination of protective devices.

The protection of islanded distribution system has been discussed in [5] and [6]. It has been shown that due to low fault currents, most of the conventional protection principles fail to provide reliable protection, except the differential protection system. It is also mentioned in [6] that the differential scheme is not cost-effective in distribution systems. So, a protection system in islanded distribution systems is needed that is economical and also reliable.

Although the purely positive sequence and current limited response of inverters create difficulties for protection related functions, sequence *voltages* are created by the

system in response to faults, and they *do* appear at the inverter terminals, regardless of the inverter design. Therefore, the proposed approach explores the use of sequence *voltages* at inverter terminals for fault detection, classification, and location. Location of fault will depend on measurements available at different system locations. Distribution systems typically do not have such measurements at all buses. Therefore, the paper explores the possibility of locating faults in a 100% IBR based islanded using measurements only at the inverter terminals.

The sequence components of voltage at the POI (Point of Interconnection) of the IBRs for detection, classification, and location of fault has not been discussed in the literature. In this thesis the sequence components of voltages for different kinds of faults will be analyzed in order to detect and classify a fault, and an attempt will be made to approximately locate the fault, all from *local* measurement of voltages at the IBR terminals, and using sequence components of these voltages. Chapter 2 will describe the models and the system used for this study. It will show operational anomalies of 100% IBR based systems compared to traditional systems in terms of boundary conditions used for traditional fault analysis. Chapter 3 will focus on simulation of the system described in Chapter 2, and using the results to create fault detection and classification methods. Chapter 4 will describe an attempt to use machine learning on local sequence voltage data to approximately locate the faulted feeder. Chapter 5 will present observations/conclusions from the study and outline future work.

Chapter 2

Models and Methodology

The 4.16 kV IEEE 13-bus distribution system [7] shown in Figure 2.1 is modeled in PSCAD and has been used for simulations. The grid source in the figure is isolated and replaced by a grid forming inverter. Three grid following inverters are connected as shown in the figure. Table 2.1 shows the ratings of these inverters, as well their interconnecting transformers specifications.

Inverter	Voltage Rating(kV)	Power Rating(kVA)	Transformer Connection	Transformer Primary/Secondary Voltages(kV)
INV1	0.48	1500	Δ-YG	0.48/4.16
INV2	0.48	1000	Δ-Y	0.48/4.16
INV3	0.48	800	Δ-Y	0.48/4.16
INV4	0.48	800	Δ-Y	0.48/4.16

Table 2.1: Inverters and their Interconnecting Transformer Specifications

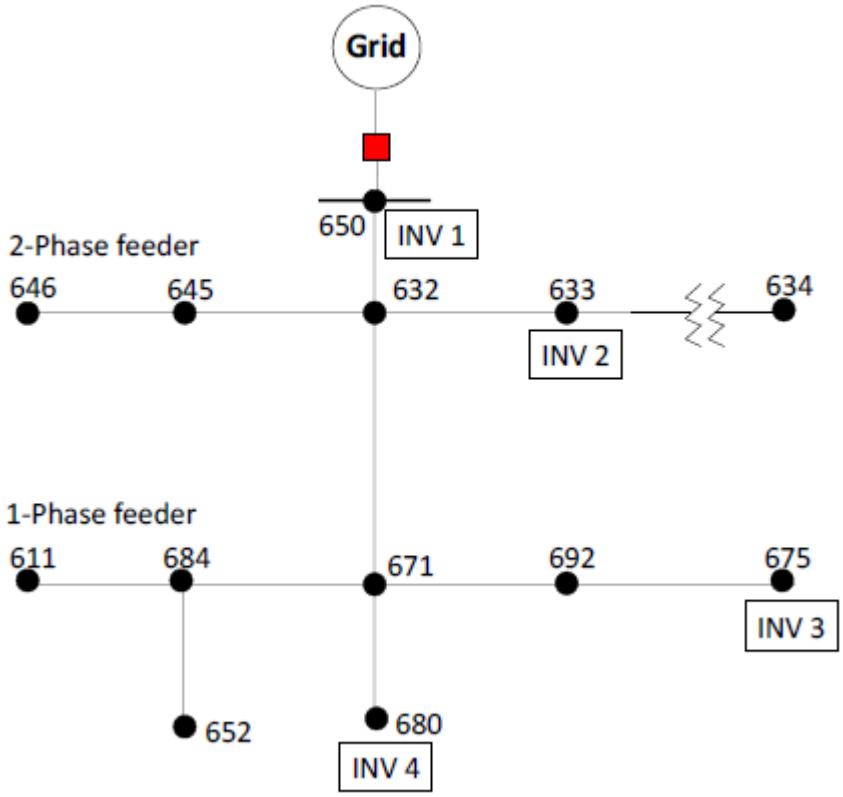

Figure 2.1: Single line diagram of IEEE 13-bus system fed by four inverters [7]

In the distribution system of Figure 2.1, INV1 is a grid forming inverter, providing both positive and negative sequence currents while INV2, INV3 and INV4 are grid following inverters that block the negative sequence currents [7]. In this case where it is an islanded distribution system and there is no synchronous generator, INV1 plays the role of a synchronous generator to maintain the voltage and frequency reference to the grid following inverters (INV2, INV3 and INV4).

There is a 600 kVar three phase capacitor bank at bus 675 and a 100 kVar single phase capacitor bank at bus 611. Capacitors are providing partial reactive power in the islanded distribution system. Rest of the reactive power, and all real power are supplied by the four inverters by a robust power sharing mechanism. In addition, since the distribution systems are unbalanced, capacitors are also contributing some amount

of zero sequence current and negative sequence current [5] along with INV1 during normal operation and during faults. The total load on the system is 3158+j1588 kVA (total 3534 kVA) including capacitor banks, which can be fed by the inverters without grid support, as their total capacity is 4100 kVA.

2.1 Inverter Model

In the distribution system of Figure 2.1, the load power is shared among all inverters. Inverters use a robust universal PQ droop control method to share the load among each other without any communication and irrespective of the X/R ratio of the network [8] . The inverter model uses a Proportional Integral(PI) controller in the synchronous reference frame (dq coordinates), faithfully representing commercial inverters. The control diagram of inverters is shown in Figure 2.2.

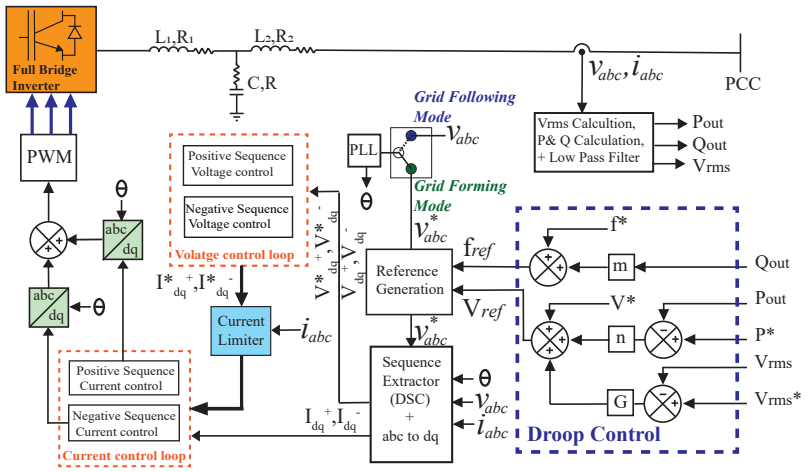

Figure 2.2: Inverter control diagram with PI Controller [8]

Depending on the switch position, the control diagram of the inverter works in the grid following mode or grid forming mode. In the grid following mode, the voltage and frequency references are generated by the robust PQ droop control, which though

counter intuitive, is shown to perform better than the conventional droop control[9, 10]. Reference voltage v^*_{abc} is formed based on these values. In grid forming mode, the reference voltage is created by the inverter itself, as it is supposed to provide grid-function. The controls work in the synchronous dq reference frame on the sequence components of actual and observed voltages and currents. In essence, the voltage control block nullifies the negative sequence voltage by providing a zero reference to the negative sequence dq value for grid forming inverters (allowing negative sequence currents to flow), whereas the current control block suppresses the negative sequence currents by providing a zero reference to the negative sequence current in dq frame for grid following inverters. The control block is described in details in the following paragraphs.

The IEEE 13-bus distribution system used for the simulation has an unbalance in load, phase, and feeder impedance. Therefore, a grid forming inverter is needed to balance the voltages and provide a voltage and frequency reference like a grid for the other conventional grid following inverters. The inverters have been modeled as recommended by the National Renewable Energy Laboratory (NREL) report on commercial inverters [11]. The current is limited to 1.2 pu of their rated current. Figure 2.3 shows the INV1 currents during a line to ground(AG), which are unbalanced and limited to 1.2 pu during fault.

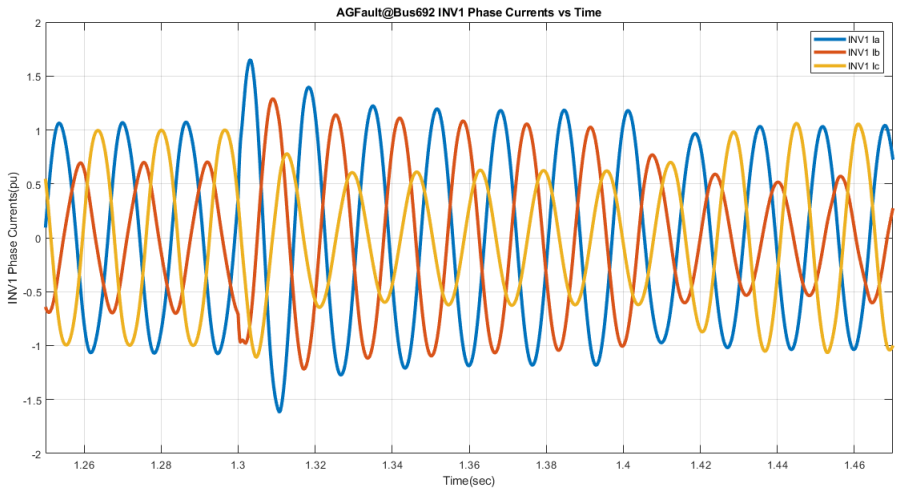

Figure 2.3: INV1 Phase Currents for a line to ground fault(AG) at bus 692

The design difference between the grid forming inverter and grid following inverters is that the grid forming inverter operates in Negative Sequence Voltage Blocking(NSVB) mode and allows negative sequence current to flow to balance the voltages in the system. As a result, INV1 provides unbalanced currents to maintain the voltage. However, grid following inverters operate in Negative Sequence Current Blocking(NSCB) which blocks negative sequence current, and can only supply balanced positive sequence current. Also, grid forming inverter generates an internal reference of three-phase balanced voltages at the system frequency. In contrast, the grid-following inverters follow the voltages measured at their terminal and use their terminal voltage for reference [7]. Figure 2.4 shows the negative sequence current of grid forming inverter(INV1) and grid following inverter(INV2) for the same line to ground fault. The behaviour of INV3 and INV4 is similar to INV2.

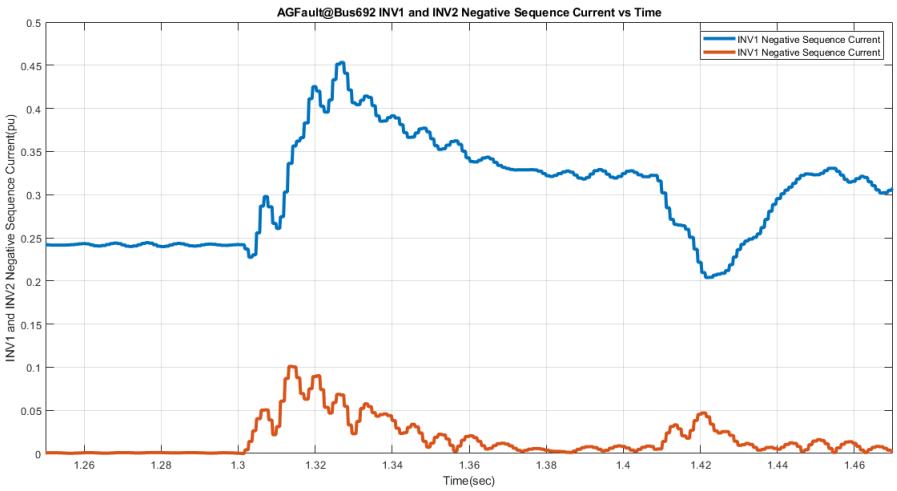

Figure 2.4: INV1 and INV2 Negative sequence currents for a line to ground fault at bus 692

As Figure 2.4 shows, only INV1 provides negative sequence current while INV2 blocks negative sequence current. None of the inverters can supply zero sequence currents as they are not grounded. There is only one zero sequence source chosen in the system, which is the secondary terminal of Δ/YG transformer connecting INV1 to the system. This is done to produce the most stringent conditions for fault detection at the grid following inverters, since only limited positive sequence current will be available at their terminals.

The droop control in the inverter's control diagram (Figure 2.2) produces reference values V_{ref} and f_{ref}. The P_{out}, Q_{out}, V_{rms} passe through a low pass filter to remove all the low-order harmonics and increase the PI controller's disturbance rejection capability [8]. PLL (Phase Locked Loop) is required to lock on to the grid and generate θ for conversion of natural reference frame (abc coordinates) to synchronous reference frame(dq coordinates) via DSC block[8].

The inverter uses Delayed Signal Cancellation(DSC) method to decompose $vabc$ or v^*_{abc} into its negative sequence and positive sequence voltage and then convert them to

their respective dq quantities. The control diagram of inverters has two separate PI controllers for voltage and current (Voltage Control Loop and Current Control Loop shown in Figure 2.2). The voltage control loop contains positive and negative sequence control, which works based on the PI control mechanism. The output of positive sequence voltage control is the reference input for positive sequence current control, and the output of negative sequence voltage control is reference for the negative sequence current control. Before passing to the current control loop, the current is limited by a current limiter to protect the inverter's components during overload and fault. The output of the current loop is controlling PWM signals of the Voltage Source Inverter (VSI). Finally, the output of the inverter passes through an LCL filter to decrease the high-switching frequency ripple.[8]

When the switch in Figure 2.2 is in grid forming mode or in NSVB mode, the inverter uses Delayed Signal Cancellation(DSC) method to decompose $vabc$ and v^*_{abc} into its negative sequence and positive sequence voltage and then converts them to their respective dq quantities. v^*_{abc} is reference voltage which grid forming inverters sets at its terminal. The inverter in grid forming mode tries to match the reference variables and bring the negative sequence voltage steady state to zero to balance the voltages.[8] Figure 2.5 shows the voltage in grid forming inverter(INV1) provides 1 pu balanced voltage before fault as commanded in the inverter control diagram.

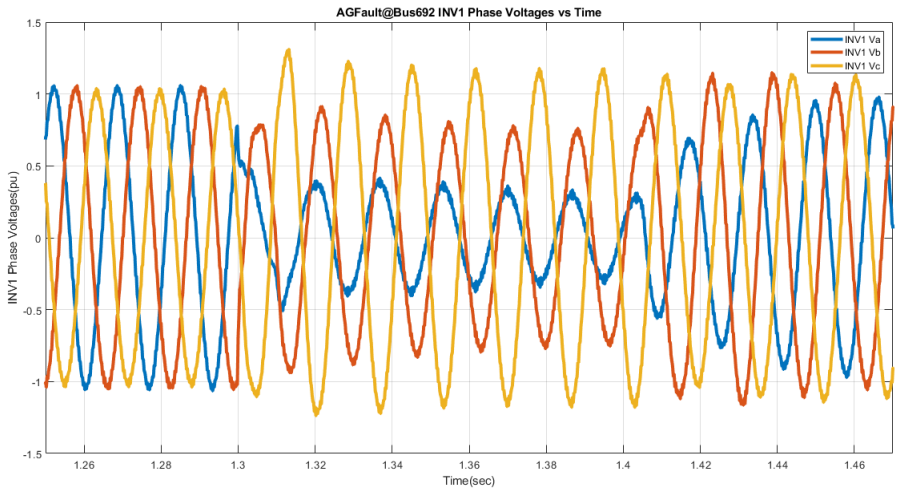

Figure 2.5: Grid forming(INV1) phase voltages for a line to ground fault at bus 692

When the switch in Figure 2.2 is in grid following mode or NSCB mode, voltage reference for grid following inverters are v_{abc}, the terminal voltage of the inverter. After the voltage and current have been changed to their respective dq quantities using the DSC block, the voltage control loop provides an output current reference. The output currents $iabc$ are compared with the positive sequence reference currents i^*_{abc} in order to block negative sequence current. The PI controller has two separate current controllers (positive sequence current control and negative sequence current control). The negative sequence current control compares negative sequence output current I^-_{dq} with a zero reference and positive sequence current control compares the positive sequence output current I^+_{dq} with the I^{+*}_{dq} [8]. The result of current control loop is changed back to natural reference frame (abc coordinates) and is an input to the inverter's drive system or PWM (Pulse Width Modulation) signals. Figure 2.4 shows the negative sequence current of INV2 is blocked, as INV2 is a grid following inverter. In addition, INV2 voltage is balanced and follows INV1 voltages during the healthy phase of the system(shown in Figure 2.6). INV3 and INV4 voltages are similar to INV2 as they are also grid following inverters.

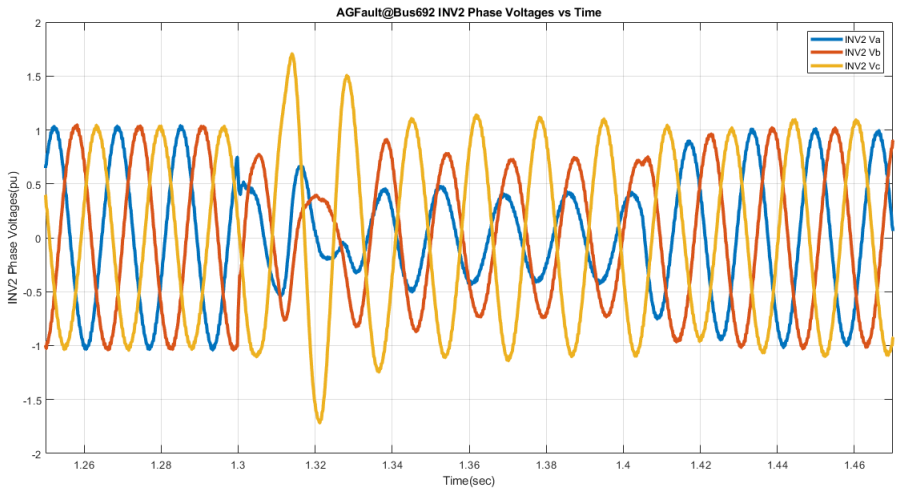

Figure 2.6: Grid following(INV2) phase voltages for a line to ground fault at bus 692

2.2 Methodology

Reference [6], has concluded that besides differential protection, two protection systems work to detect faults at inverter terminals in islanded distribution systems. They are undervoltage relay and zero sequence overcurrent relay. The problem with the differential protection scheme is that it is costly for distribution systems. Zero sequence overcurrent relay works reliably for ground faults. The condition for which the zero sequence overcurrent relay works is if the grid side of the interconnecting transformer provides a zero sequence current source. However, if the transformer connection is Δ/Y instead of Δ/YG, then zero sequence overcurrent relay does not work, which is the case for the system under study. Thus, only undervoltage based fault detection and classification remains to be explored. However, it was observed in [6] that undervoltage based detection is not reliable for remote faults. That is why this thesis attempts a sequence component based approach, as sequence voltages are likely to be more sensitive to different types of faults than phase voltages. However, fault analysis is required for this approach.

2.2.1 Fault Model

In order to observe if the traditional fault model with boundary conditions holds for an unbalanced island fed by IBRs, faults were created on this system. The simulation results show that the fault behavior is significantly different in the islanded system. In boundary conditions of traditional distribution system, the load current is neglected, and an ideal case for the voltages is assumed. This holds because the fault current is much higher than the load current in traditional distribution systems. For the same reason, the phases which are not affected by the fault can be assumed to remain at their pre-fault values. Since IBRs limit the fault current in the islanded distribution systems, the assumption of neglecting load current does not hold, because the load current and fault current do not differ considerably.

Table 2.2 and Table 2.3 show the sequence voltages at fault point for a traditional distribution system, assuming boundary conditions for different fault resistances for a line to ground fault and double line to ground fault, respectively. The symmetrical sequence components of voltages can be calculated using Equation 2.1. In equation 2.1 the complex number a and a^2 is defined by equation 2.2 and equation 2.3, respectively.

$$\begin{bmatrix} V_0 \\ V_1 \\ V_2 \end{bmatrix} = \frac{1}{3} \begin{bmatrix} 1 & 1 & 1 \\ 1 & a & a^2 \\ 1 & a^2 & a \end{bmatrix} \tag{2.1}$$

$$a = e^{j\frac{2pi}{3}} = -\frac{1}{2} + j\frac{\sqrt{3}}{2} \tag{2.2}$$

$$a^2 = e^{-j\frac{2pi}{3}} = -\frac{1}{2} - j\frac{\sqrt{3}}{2} \tag{2.3}$$

In traditional distribution systems, as shown in Table 2.2 and Table 2.3, it is assumed

Boundary Conditions		V_0(pu)	V_1(pu)	V_2(pu)
$V_a = 0$ pu $V_b = 1\angle -120°$ pu $V_c = 1\angle 120°$ pu	$Rf = 0$	$0.\bar{3}$	$0.\bar{6}$	$0.\bar{3}$
$V_a = 0.1$ pu $V_b = 1\angle -120°$ pu $V_c = 1\angle 120°$ pu	$Rf \neq 0$	0.3	0.7	0.3
$V_a = 0.2$ pu $V_b = 1\angle -120°$ pu $V_c = 1\angle 120°$ pu		$0.2\bar{6}$	$0.7\bar{3}$	$0.2\bar{6}$

Table 2.2: Fault point sequence voltages for a single line to ground(AG) in traditional distribution system

Boundary Conditions		V_0(pu)	V_1(pu)	V_2(pu)
$V_a = 0$ pu $V_b = 0$ pu $V_c = 1\angle 120°$ pu	$Rf = 0$	$0.\bar{3}$	$0.\bar{3}$	$0.\bar{3}$
$V_a = 0.1$ pu $V_b = 0.1$ pu $V_c = 1\angle 120°$ pu	$Rf \neq 0$	0.3055	0.3512	0.3512
$V_a = 0.2$ pu $V_b = 0.2$ pu $V_c = 1\angle 120°$ pu		0.2906	0.3712	0.3712

Table 2.3: Fault point sequence voltages for a double line to ground(ABG) in traditional distribution system

that the voltages which are not affected by the fault will remain at their pre-fault values, and this assumption is correct. However, by looking into the actual voltages and sequence voltages of faults at the fault point in islanded distribution systems, the difference between traditional and islanded distribution system can be observed. Table 2.4 and Table 2.5 show actual voltages and sequence voltages at the fault point for line to ground and double line to ground fault in the IEEE 13-bus system. The fault resistance in the tables is 0.1 ohms.

Fault Bus	V_0(pu)	V_1(pu)	V_2(pu)	V_a(pu)	V_b(pu)	V_c(pu)
Bus 692	0.1851	0.621	0.4843	0.03795	1.175	0.7367
Bus 680	0.2192	0.6392	0.4723	0.03588	1.212	0.7295
Bus 633	0.1206	0.6013	0.5027	0.0391	1.098	0.8069
Bus 671	0.1851	0.621	0.4843	0.03806	1.16	0.7367

Table 2.4: Fault point sequence voltages for a line to ground(AG) in different buses of an islanded distribution system

Fault Bus	V_0(pu)	V_1(pu)	V_2(pu)	V_a(pu)	V_b(pu)	V_c(pu)
Bus 692	0.2205	0.2394	0.2196	0.02438	0.04071	0.6743
Bus 680	0.2455	0.2634	0.2433	0.02193	0.0392	0.7483
Bus 633	0.1688	0.1869	0.1695	0.02902	0.04506	0.5243
Bus 671	0.2205	0.2394	0.2196	0.02438	0.04169	0.6743

Table 2.5: Fault point sequence voltages for a double line to ground(ABG) in different buses of an islanded distribution system

As seen in Table 2.4, for phase A to ground fault in the islanded distribution system, the unaffected phase voltages (phase B and phase C in this case) change considerably - phase B voltage could go as high as 1.175 pu, and phase C voltage could go as low as 0.7367 pu. In traditional distribution system, for a phase A to ground fault the phase B and Phase C voltage don't change much; that is why they are assumed so in the boundary conditions. Likewise, for double line to ground (ABG) fault, it is expected that phase C voltage does not change in traditional distribution systems, but as table 2.5 shows, for a ABG fault in the islanded distribution system, phase C voltage could go as low as 0.5243 pu. This shows that sequence voltages of traditional and islanded distribution system are markedly different and the traditional fault model cannot be assumed in the system under study. This is an important observation that changed the course of this thesis. Sequence voltages had to be obtained by extensive fault studies performed in PSCAD, rather than obtaining them using traditional phasor domain methods for unbalanced systems. Chapter 3 shows how such simulations were performed and how different thresholds for fault detection and classification depended on the simulation results.

Chapter 3

Simulated System and Results

The underlying rationale behind this work is that undervoltage relays placed at the inverter terminals are not fully reliable in detecting faults under islanded conditions. In addition, they cannot be used for fault classification and location. This chapter shows simulation results to support this rationale and shows how sequence voltage based fault detection and classification is feasible and reliable.

Analyzing the 13-bus islanded distribution feeder in PSCAD, it was observed that the undervoltage based detection works well to detect faults at all buses except for one remote bus (bus 634). The bus is a 480 V bus fed by a 500 kVA, 4.16 kV/0.48 kV distribution transformer. Table 3.1 shows the phase voltages at INV1 during different faults at bus 634. Voltages at INV2, INV3, and INV4 show a similar pattern as the INV1 voltages.

Type of Fault	INV1 Phase a Voltage(pu)	INV1 Phase b Voltage(pu)	INV1 Phase c Voltage(pu)
AG	0.8725	1.066	0.999
ABG	0.9156	0.911	0.9873
ABCG	0.7592	0.7786	0.7175
AB	0.8265	0.7703	1.097

Table 3.1: INV1 voltages for different types of faults at bus 634

As can be observed from Table 3.1, the inverter voltages for remote fault are not suppressed enough to reliably detect faults with an undervoltage threshold. In a larger distribution system this could also pose problems at more than one remote locations. Therefore, undervoltage based detection cannot be reliably applied in general for fault detection. It is also clear from the table that fault classification can also not be reliably performed, as proper and clear discrimination between fault-voltages is not available. On the other hand, since sequence voltages will be closely tied to fault-types, sequence voltage based detection and classification is likely to provide better sensitivity for all faults, including remote faults. This chapter investigates this hypothesis through simulation results and provides a methodology for sequence voltage based detection and classification of faults.

3.1 Detection of Faults Using Sequence Voltages

The most restrictive topology is assumed in this study - 1) voltage measurements are assumed available only at the point of interconnection (POI) of IBRs, 2) positive sequence currents are limited to 1.1 pu of the rated current, 3) zero sequence source is only provided at the grid forming inverter, rendering zero sequence current based fault detection impossible at all other inverter terminals. Measured voltages are converted to sequence voltages and these sequence values are used for fault detection and classification.

3.1.1 Zero Sequence Voltage

Fault analysis was performed at all buses of the IEEE 13-bus system. Four kinds of faults - single line to ground (AG), double line to ground (ABG), line to line (AB)

and three phase to ground (ABCG) were created. The zero sequence voltages at inverters for different faults at all buses were observed. Figures 3.1-3.4 show zero sequence voltages seen by INV1 for AG, ABG, ABCG and AB faults at bus 692 (selected for illustration). INV2, INV3 and INV4 experience a similar pattern of zero sequence voltages as INV1. In all simulations and figures, the fault occurs at 1.3 s for a duration of 0.1 s with a fault resistance of 0.1 Ω. The fault is cleared by PSCAD at 1.4 s by changing the input control signal to the fault model. The RMS values of phase and sequence components were calculated using the FFT block of PSCAD, which calculates the frequency of the input time-domain waveform, extracts the fundamental components of phasors and converts them to sequence components. Some of the values plotted in the figures that follow do show a small variation in the values during fault, which are possibly due to inadequate frequency tracking by the PSCAD FFT block. They are also due to the fact that some faults do not stabilize within the time-period chosen for fault. These variations are not present in all plots and are not significant.

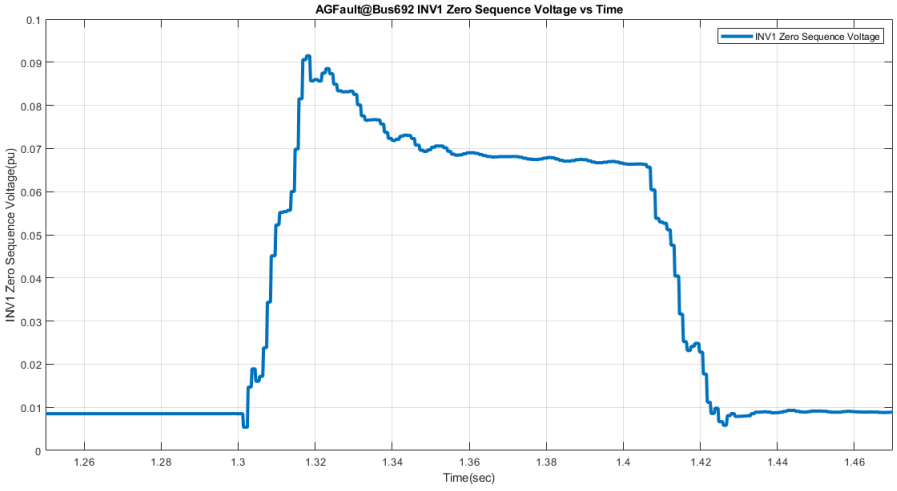

Figure 3.1: INV1 zero sequence voltage for AG fault at bus 692

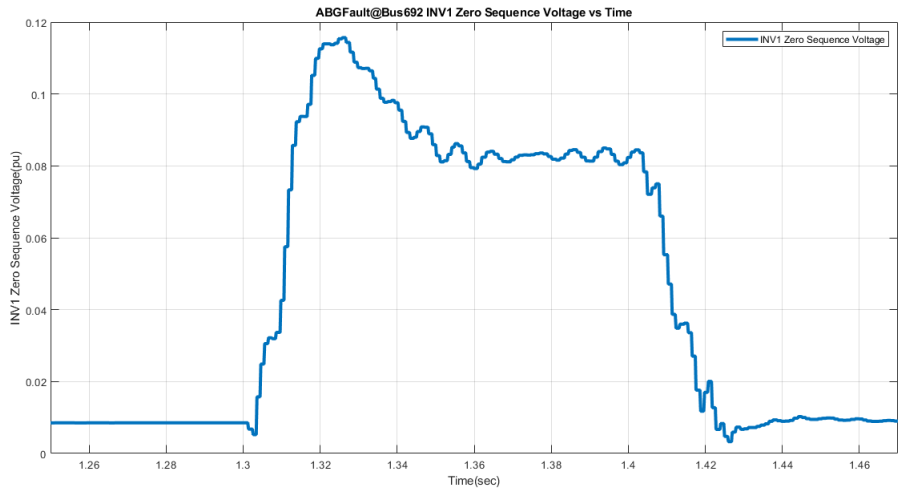

Figure 3.2: INV1 zero sequence voltage for ABG fault at bus 692

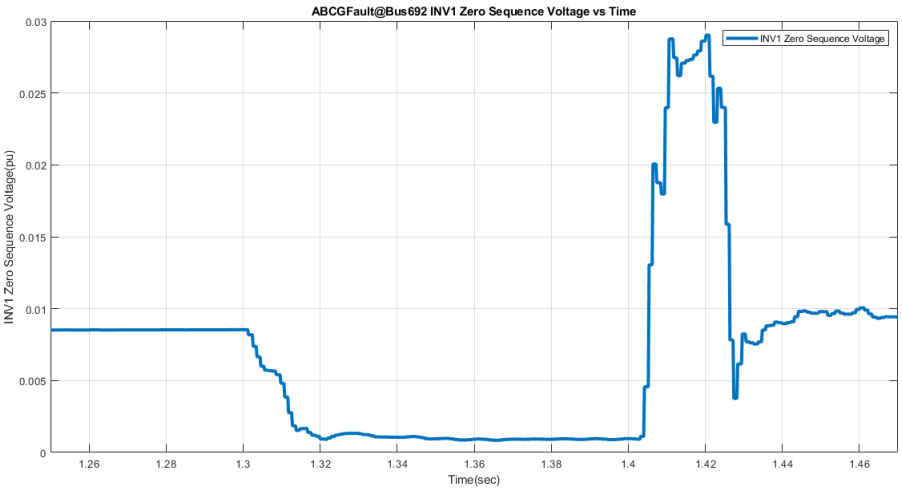

Figure 3.3: INV1 zero sequence voltage for ABCG fault at bus 692

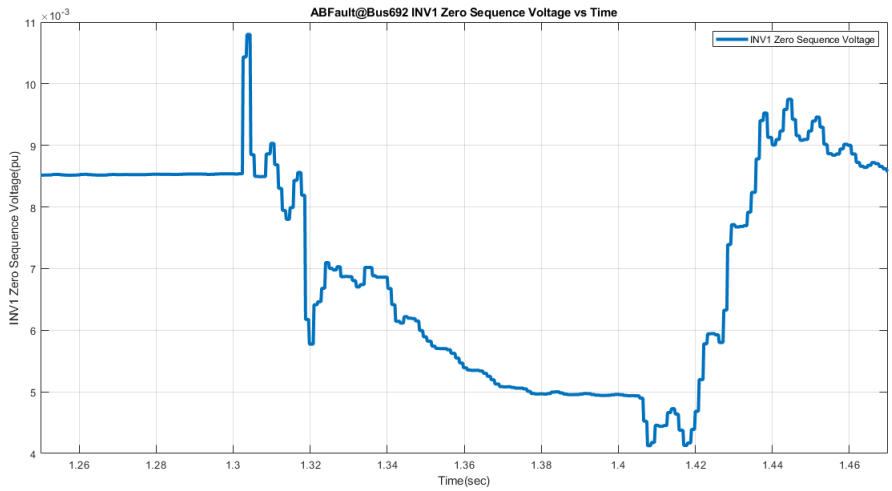

Figure 3.4: INV1 zero sequence voltage for AB fault at bus 692

As seen in the figure 3.1-3.4, zero sequence voltage increases compared to its pre-fault value for line to ground and double line to ground faults and decreases compared to its pre-fault value for three phase to ground and line to line faults. This is expected. So, zero sequence voltage can be used to detect line to ground and double line to ground faults at all buses of IEEE 13-bus system. Even at the remote fault at bus 634, Figure 3.5 shows the zero sequence voltage at INV1 increases significantly. Voltages INV2, INV3, and INV4 show similar behavior.

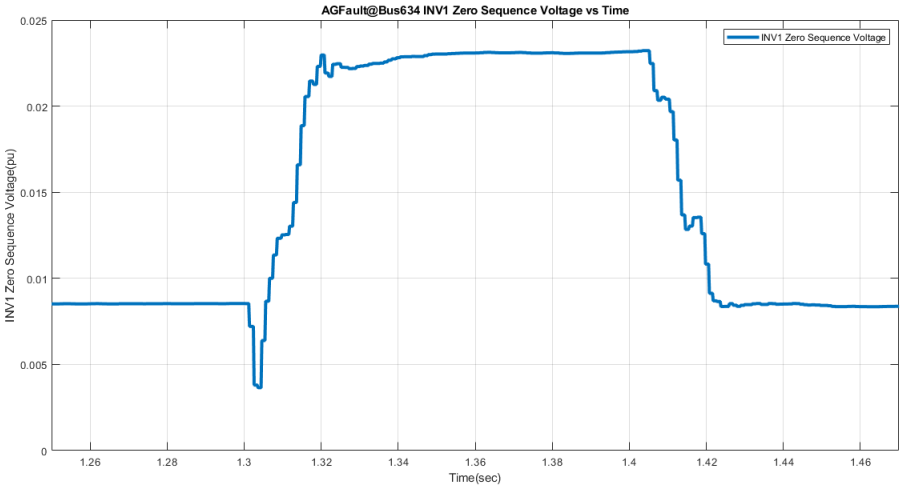

Figure 3.5: INV1 Zero sequence voltage for AG fault in bus 634

Measured values for zero sequence voltage at INV1 from the Figure 3.5 before and after a AG fault at bus 634 are shown in Table 3.2. Clearly, a threshold of 200% can be applied to detect AG faults in this system.

Type of Fault	V_a(pu)	V_b(pu)	V_c(pu)	V_0(pu)	Increase in V_0(%)
Before Fault	1.031	1.014	0.9991	0.00853	270
After Fault	0.8725	1.066	0.999	0.02312	

Table 3.2: INV1 Zero sequence voltage before and after a single line to ground (AG) fault at bus 634

However, for a double line to ground (ABG) fault at bus 634, although zero sequence voltages at INV1 and INV2 increase, the zero sequence voltages at INV3 and INV4 do not increase significantly enough to apply the threshold chosen for the LG fault reliably. It was observed that the pre-fault zero sequence voltages at these inverters are more than twice the zero sequence voltages at INV1 and INV 2. This is due to the fact that there is a Wye-grounded capacitor bank right at the bus where INV3 is connected (bus 675), which provides local zero sequence currents and lifts the pre-fault zero sequence voltage of the surrounding buses. This shows that the pre-fault voltages are not well-balanced, as they should be in the islanded case. This is a design issue. This is considered a practical issue and it will be further explored and resolved in section 3.3.

3.2 Positive Sequence Voltage

Positive sequence voltage is is expected to decrease for all faults. Figure 3.6, 3.7, 3.8, and 3.9 show the positive sequence voltages at INV1 terminal for AG, ABG, ABCG and AB faults, respectively, on bus 692. INV2, INV3 and INV4 experience a similar pattern of positive sequence voltages as INV1. As the Figures 3.6-3.9 show, the positive sequence voltage at inverters decrease significantly during fault for all types

of fault at bus 692. Positive sequence voltages at inverters decrease significantly for a ABCG faults even at bus 634, as seen in Figure 3.10. Positive sequence voltage can therefore be used to detect three phase to ground fault at bus 634.

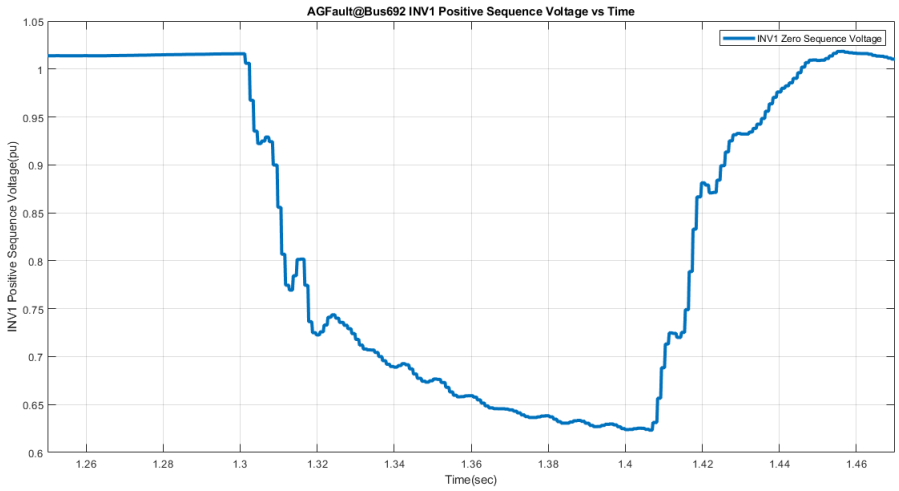

Figure 3.6: INV1 positive sequence voltage for AG fault at bus 692

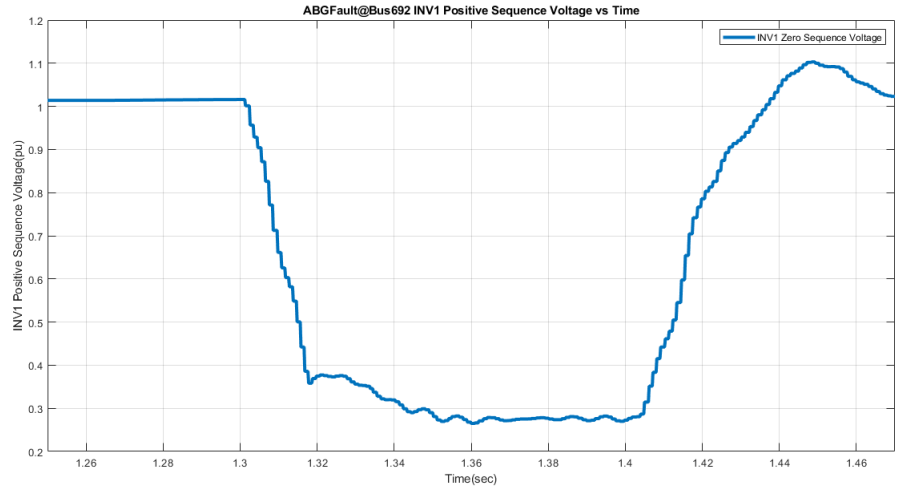

Figure 3.7: INV1 positive sequence voltage for ABG fault at bus 692

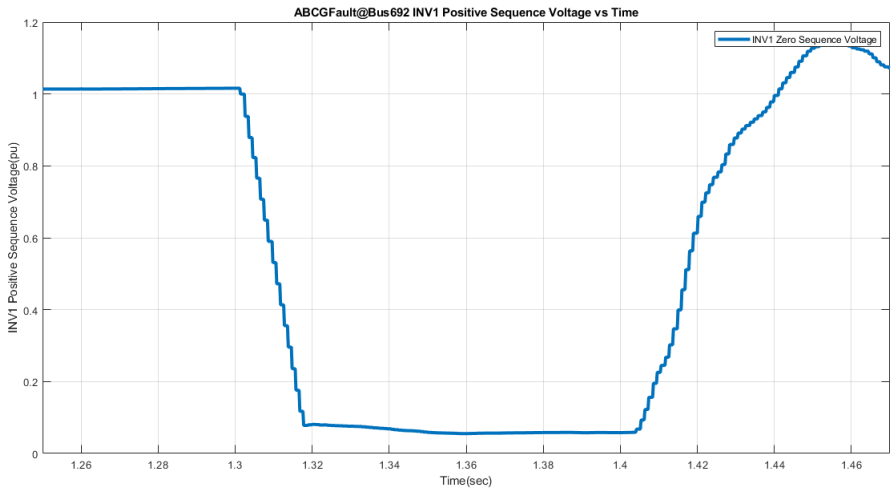

Figure 3.8: INV1 positive sequence voltage for ABCG fault at bus 692

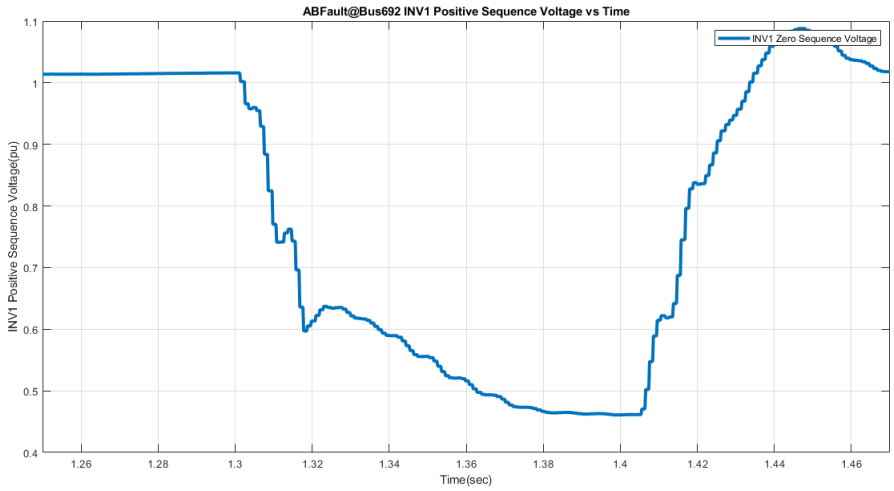

Figure 3.9: INV1 positive sequence voltage for AB fault at bus 692

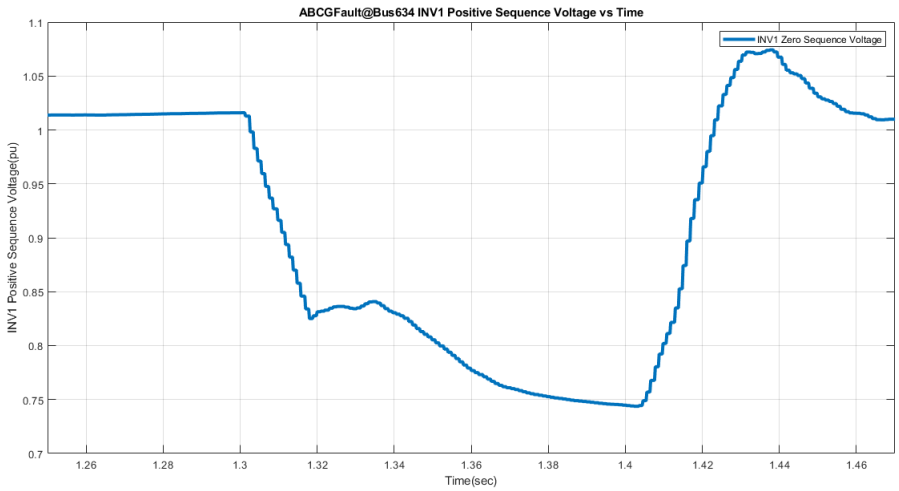

Figure 3.10: INV1 Positive sequence voltage for ABCG fault at bus 634

Based on Figure 3.10, the exact values of the positive sequence of voltage of INV1 before and after a three phase to ground fault at bus 634 can be found. These exact values are shown in Table 3.3. Based on this table, a three phase to ground fault in the system can be detected with a threshold of 0.8 pu, or 80%.

Type of Fault	V_a(pu)	V_b(pu)	V_c(pu)	V_1(pu)	Decrease in V_1(%)
Before Fault	1.031	1.014	0.9991	1.015	74
After Fault	0.7592	0.7786	0.7175	0.7495	

Table 3.3: INV1 positive sequence voltage before and after three phase to ground fault at bus 634

3.3 Negative Sequence Voltage

Figures 3.11-3.13 show the negative sequence voltages at inverter INV1 for a AG, ABG, and AB fault, respectively, at bus 692. Values at INV2, INV3 and INV4 exhibit similar behavior. It is seen that the negative sequence voltage at inverters increase the most - even more than zero sequence voltages. It is a good sign for detecting faults. It shows that negatives sequence voltage can be used to detect *all* unbalanced faults

(line to ground, line to line and double line to ground). Thus, a negative sequence voltage based threshold is preferred in this work to detect all unbalanced faults.

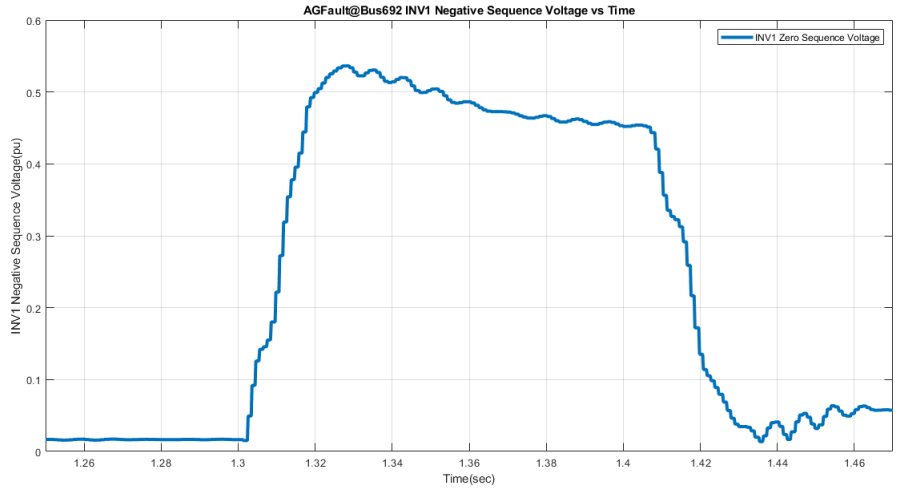

Figure 3.11: INV1 negative sequence voltage for AG fault at bus 692

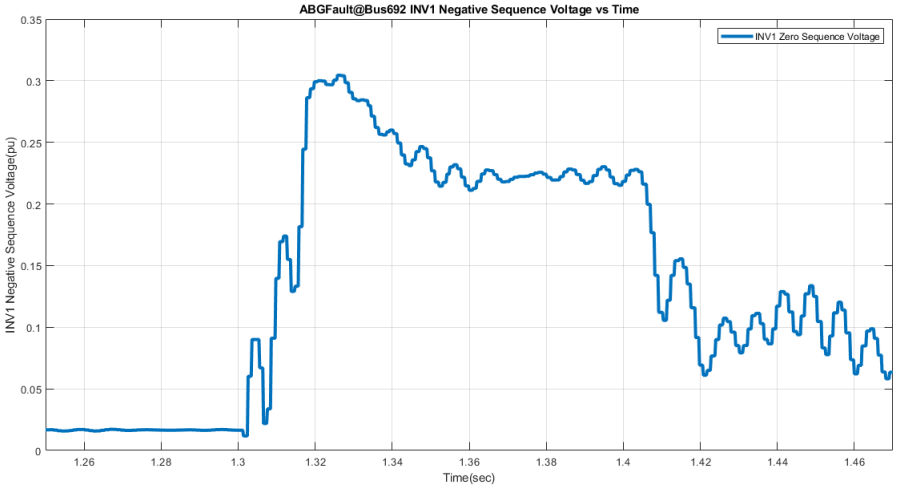

Figure 3.12: INV1 negative sequence voltage for ABG fault at bus 692

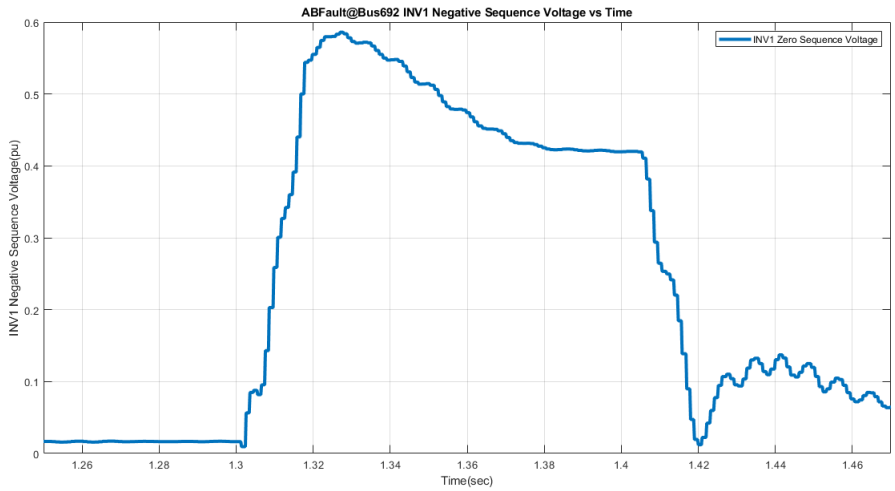

Figure 3.13: INV1 negative sequence voltage for AB fault at bus 692

Figure 3.14-3.16 show negative sequence voltage of INV1 for AG, ABG and AB fault at bus 634. Negative sequence voltage Voltage of INV2, INV3 and INV4 exhibit similar behavior.

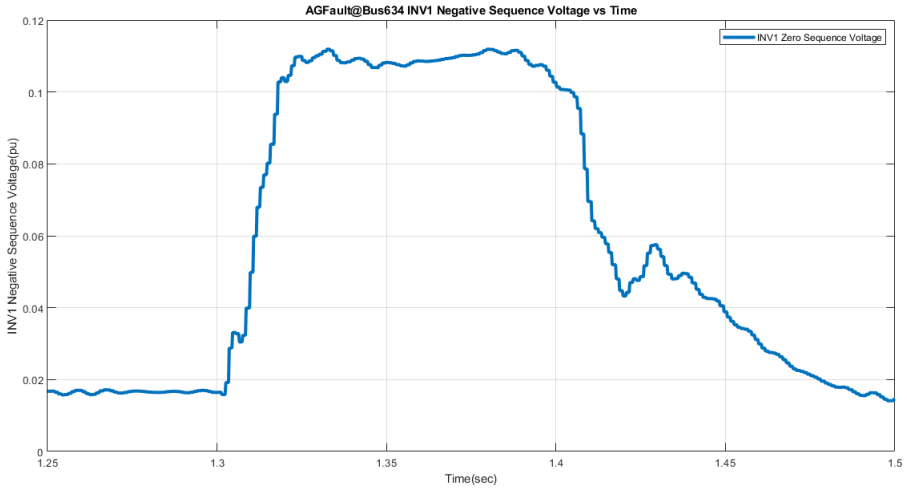

Figure 3.14: INV1 negative sequence voltage for AG fault at bus 634

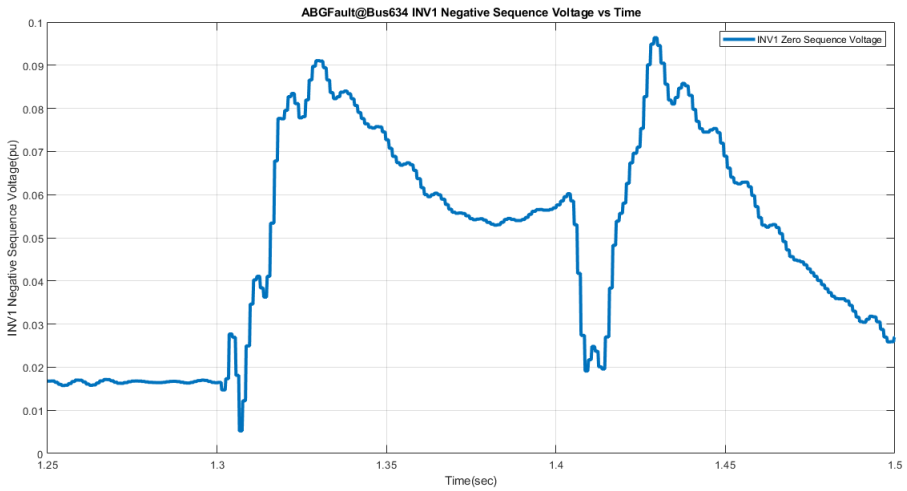

Figure 3.15: INV1 negative sequence voltage for ABG fault at bus 634

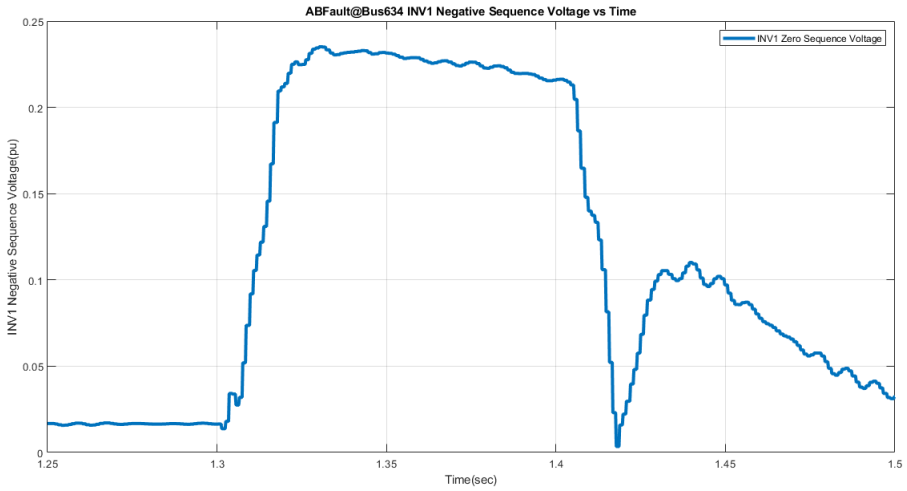

Figure 3.16: INV1 negative sequence voltage for AB fault at bus 634

From Figures 3.14 - 3.16, the exact values of the negative sequence voltage at INV1 before and during line to ground,double line to ground, and line to line fault can be found. Table 3.4-3.6 show these values.

Type of Fault	V_a(pu)	V_b(pu)	V_c(pu)	V_2(pu)	Increase in V_2(%)
Before Fault	1.031	1.014	0.9991	0.0164	680
After Fault	0.8725	1.066	0.999	0.112	

Table 3.4: INV1 negative sequence voltage before and after line to ground(AG) fault at bus 634

Type of Fault	V_a(pu)	V_b(pu)	V_c(pu)	V_2(pu)	Increase in V_2(%)
Before Fault	1.031	1.014	0.9991	0.0164	322
After Fault	0.9156	0.911	0.9873	0.053	

Table 3.5: INV1 negative sequence voltage before and after double line to ground(ABG) fault at bus 634

Type of Fault	V_a(pu)	V_b(pu)	V_c(pu)	V_2(pu)	Increase in V_2(%)
Before Fault	1.031	1.014	0.9991	0.0164	1354
After Fault	0.8265	0.7703	1.097	0.2226	

Table 3.6: INV1 negative sequence voltage before and after line to line(AB) fault at bus 634

For all the three unbalanced faults, dividing the negative sequence voltage during fault by the negative sequence voltage before fault, the increase in negative sequence voltage can be found. Tables 3.4-3.6 show that negative sequence voltage at an inverter's terminal increases less for double line to ground fault than for single line to ground and line to line faults, but still increases significantly more than the zero sequence voltage, as documented in section 3.1. This resolves the problem faced for ABG faults, as noted in section 3.1. Therefore, the threshold value for detecting ground faults will be based on the increase of negative sequence voltage, not zero sequence voltage. With a threshold of 200% for negative sequence voltage all unbalanced faults can be reliably detected.

3.4 Identification of Fault Type Based on Sequence Voltages

The sequence voltages of faults are calculated for all the four types of faults at all the buses in the IEEE 13-bus system. Ratio of the sequence voltages during fault to their pre-fault values are plotted in Figures 3.17, 3.18, 3.19, and 3.20. For unbalanced faults changes (increment) in negative and zero sequence voltage values are plotted, and for three-phase faults changes (decrement) in the positive sequence values are plotted. These plots provide the fault profile that can be used to classify faults at the IBR terminals.

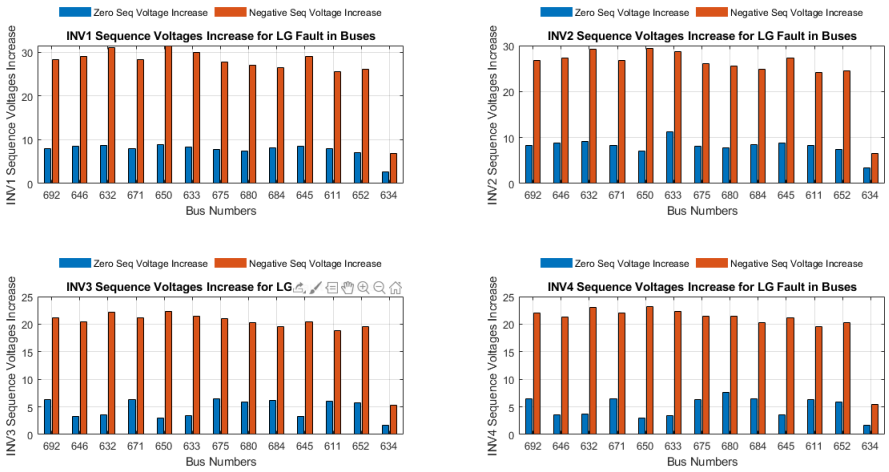

Figure 3.17: Ratio of sequence voltages observed at the four inverter-terminals after and before a line to ground fault

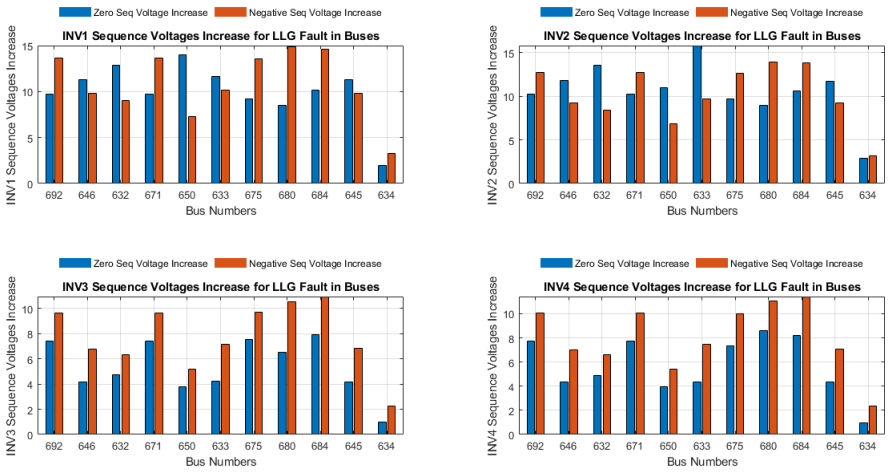

Figure 3.18: Ratio of sequence voltages observed at the four inverter-terminals after and before a double line to ground fault

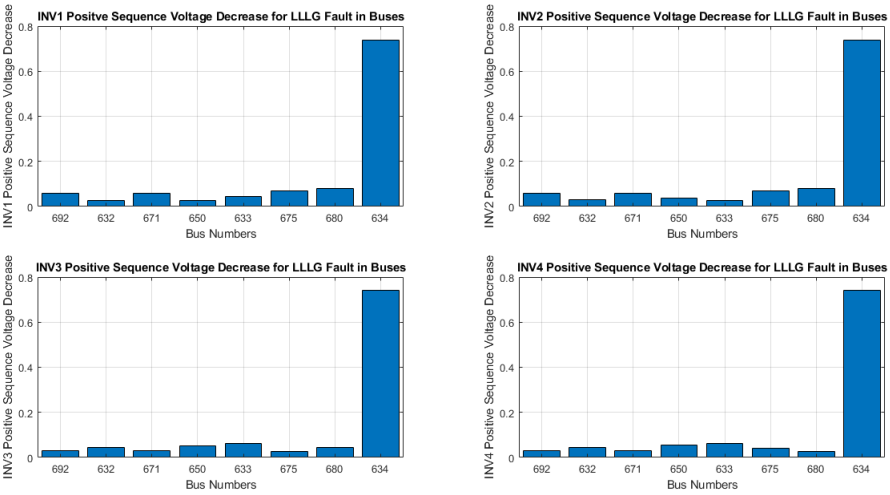

Figure 3.19: Ratio of positive sequence voltages observed at the four inverter-terminals after and before a three phase to ground fault

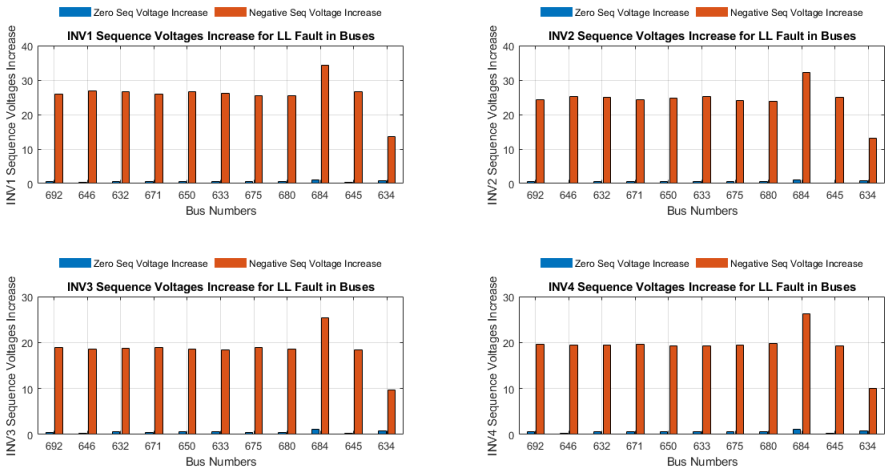

Figure 3.20: Ratio of sequence voltages observed at the four inverter-terminals after and before a line to line fault

Figure 3.21 shows the flowchart for fault detection and classification. In this figure, $\Delta V = |\frac{V_{Fault}}{V_{Pre-Fault}}| * 100\%$. As discussed in Section 3.3, fault detection thresholds are less than 80% of pre-fault positive sequence voltage to detect three phase fault, or the negative sequence voltage during fault increasing by more than 200% to detect all unbalanced faults. Once the fault is detected, a zero sequence voltage threshold is used to separate phase faults and ground faults. A negative sequence voltage threshold separates LL and LLLG faults, while a threshold of 1500% separates LG and LLG faults. This value could not have been determined without a careful observation of the sequence voltage profiles in Figures 3.17 and 3.18. For LLG faults the negative sequence voltage never exceeds 15 times its pre-fault value (for fault on bus 680), whereas the negative sequence voltage for a LG fault is never less than 18 times its pre-fault value (for fault on bus 611). Ground faults at remote bus 634 cannot be classified, though they can be detected. This bus is at the LV side (480 V) of a step-down transformer, so its main protection would be at the LV side of that transformer, not at the inverter terminals.

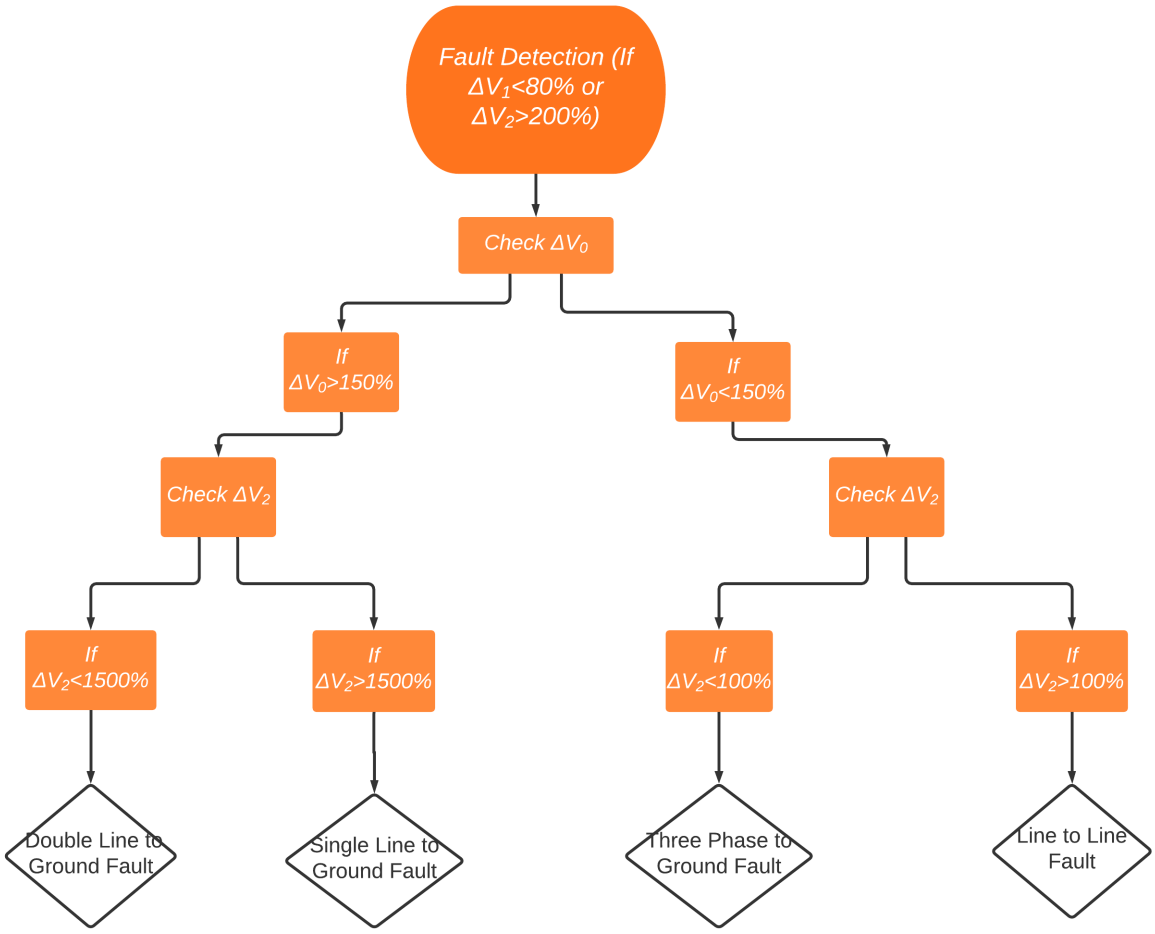

Figure 3.21: Flow chart for detecting faults and and classifying fault-type using sequence voltages

It should be mentioned that the rule based detection of Figure 3.21 works only when fault resistance is not comparable to load impedance. Faults with different fault resistances were applied to the IEEE 13-bus system. The results for line to ground fault and double line to ground fault at bus 671 (chosen for illustration) are reported in the Table 3.7 and Table 3.8. These types of faults are likely to have the largest fault resistance.

Faulted Bus	R_f	V_a(pu)	V_b(pu)	V_c(pu)	$\Delta V_0(\%)$	$\Delta V_1(\%)$	$\Delta V_2(\%)$
Bus 671	0.1	0.1833	1.087	0.8007	794	63	2841
	1	0.3657	1.089	0.9115	647	75	2330
	5	0.7838	1.101	1.005	367	94	1059
	10	0.9278	1.044	0.9767	243	97	401
	50	1.015	1.018	0.9905	121	99	103

Table 3.7: INV1 Voltages for line to ground fault at bus 671 with different fault resistances

Faulted Bus	R_f	V_a(pu)	V_b(pu)	V_c(pu)	$\Delta V_0(\%)$	$\Delta V_1(\%)$	$\Delta V_2(\%)$
Bus 671	0.1	0.1651	0.1948	0.5788	969	27	1364
	1	0.3351	0.3149	0.6215	723	40	1069
	5	0.7165	0.7185	0.8283	293	74	501
	10	0.9425	0.9525	0.9811	161	94	169
	50	1.011	1.002	0.9943	75	99	36

Table 3.8: INV1 Voltages for double line to ground fault at bus 671 with different fault resistances

Clearly the detection threshold of $V_2 = 200\%$ has to be lowered to detect the ABG fault with 10 Ω resistance; however, it can still be detected. At 50 Ω fault resistance detection is not possible. A 50 Ω fault resistance for a line to ground fault in a 4.16 kV system is equivalent to $\frac{[\frac{4160}{\sqrt{(3)}}]^2}{50}$= 115.4 kW load, so this is not surprising. This can be called a high resistance fault, and detection of such faults is not under the purview of this thesis.

Chapter 4

Identification of Fault Location Using Sequence Voltages

As mentioned in [6], the physics dictates that the voltage at the fault point be drawn to a low value; however, due to the low fault currents in islanded distribution systems, the voltages of buses are very close to each other. This creates a challenge in voltage based identification of faulted section. Since a sequence voltage based fault detection and classification approach is developed in this thesis, which is different than the phase-voltage based approach analyzed in [6], this chapter explores the possibility of identifying the faulted section based on the sequence voltages observed at in the POI of IBRs. In order to provide a metric for fault distance from the IBR, the shortest electrical fault-path between the IBR and the faulted bus is traced, and measured in terms of the feeder sections traversed by this path. For example, a fault at bus 645 is 2 sections away from INV1, 2 sections away from INV2, 4 sections away from INV3 and 3 sections away from INV4.

Sequence voltages are compared for different faults at all the buses in the IEEE 13-bus

distribution system. Figure 4.1 shows the sequence voltages for a LG fault at each bus as bar plots, with X axis marking the faulted bus, as well as the distance of the faulted bus from each inverter, shown in parenthesis. Figures 4.2-4.4 provide similar information for other three types of faults.

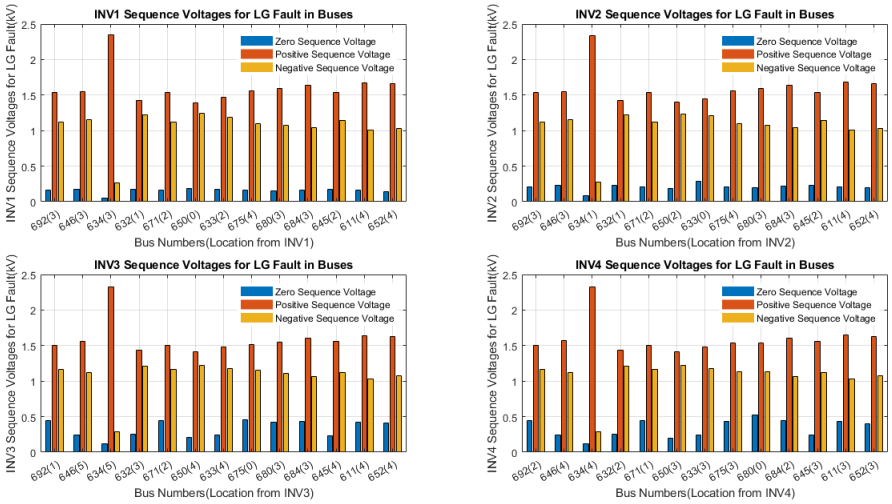

Figure 4.1: Inverters sequence voltages for single line to ground fault on all buses

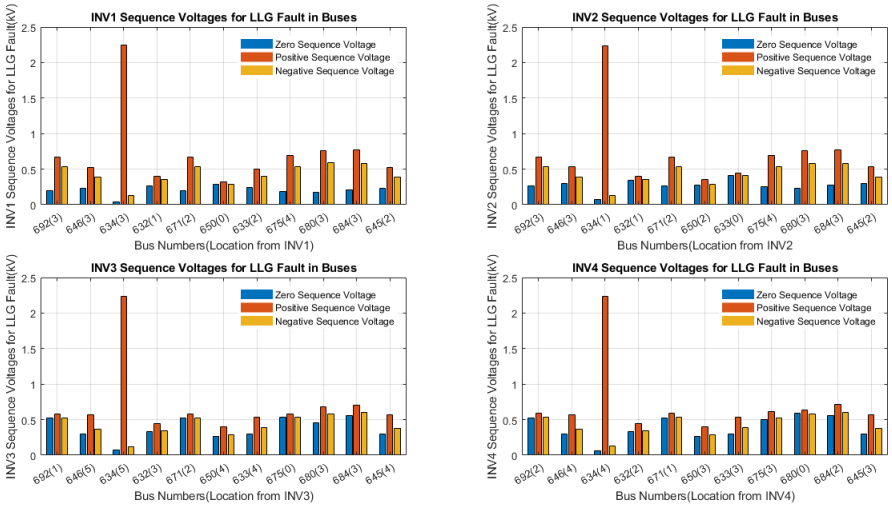

Figure 4.2: Inverters sequence voltages for double line to ground fault on all buses

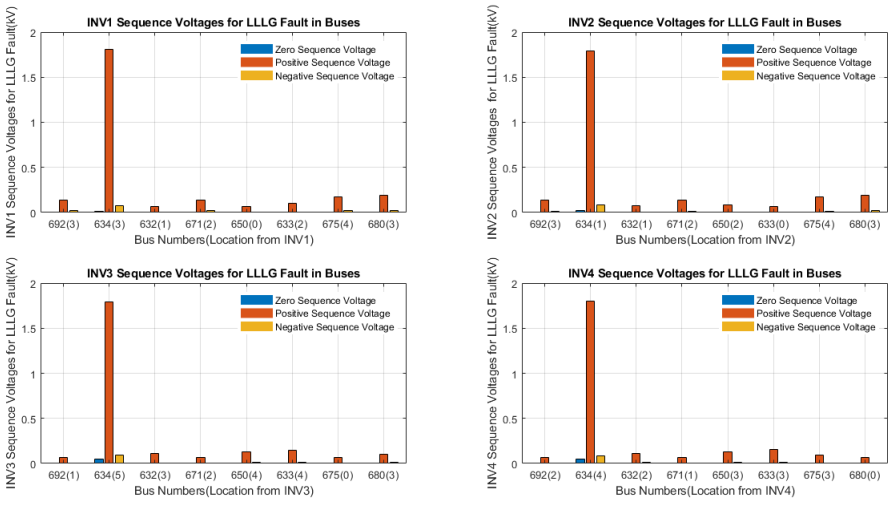

Figure 4.3: Inverters sequence voltages for three phase to ground fault on all buses

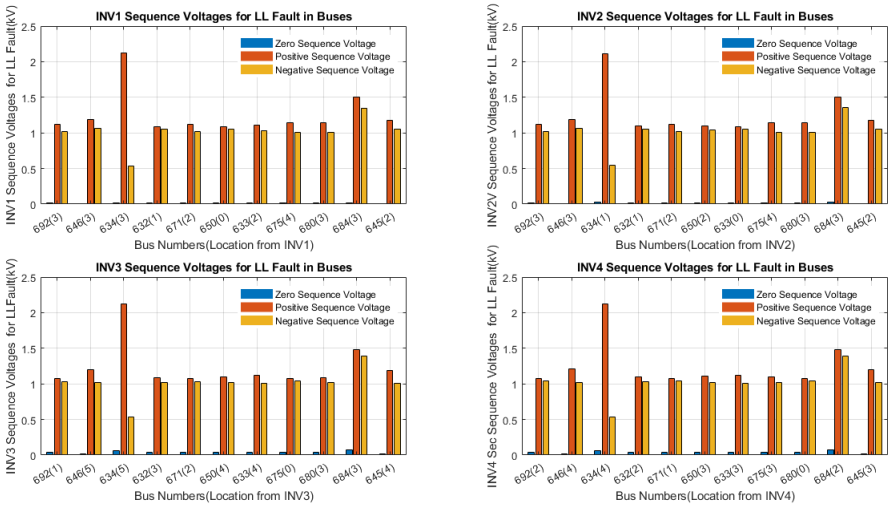

Figure 4.4: Inverters sequence voltages for line to line fault on all buses

Figures 4.1-4.4 show that at least to the naked eye it is hard to establish a correlation between sequence voltages observed at an inverter terminal and the faulted bus (or distance of the faulted bus from an inverter). For example, observe the sequence voltages at INV3 terminal in Figure 4.1 for faults at buses 675, 680 and 652, which look similar, although the buses are not equi-distant from INV3. At the same time buses 650 and 611 are equi-distant, but their sequence voltage profiles are markedly

different. Figure 4.1 shows that a single line to ground fault at bus 650, where INV1 is located, has a signature of 0.18 kV zero sequence voltage, 1.4 kV positive sequence voltage, and 1.24 kV negative sequence voltage at INV1. However, a single line to ground fault at bus 671, two feeders away from INV1, has a signature of 0.16 kV zero sequence voltage, 1.53 kV positive sequence voltage, and 1.12 kV negative sequence voltage at INV1. The differences in the sequence voltages at INV1 for a single line to ground fault at bus 650 (where INV1 is located) and 671 (which is two feeders away from INV1) is only 0.02 kV, 0.13 kV and 0.12 kV for zero, positive and negative sequence voltages, respectively, which are negligible considering the rated system voltage is 4.16 kV. These observations show that it may not be feasible to locate the faults just based on sequence voltages at IBRs.

Although the patterns of Figures 4.1-4.4 are similar, and there is little significant difference visually for locating faults based on sequence voltages, machine learning has been used to ensure that there is no hidden feature that is not being caught by visual observation. The intention is to use the sequence voltage information of Figures 4.1-4.4 as features for machine learning based classifiers to locate faults. It should be mentioned here that the increment in sequence voltages used in chapter 3 for fault detection and classification can also be used as features, but the trend in those plots were quite similar to the trend in Figures 4.1-4.4. This makes sense because the pre-fault sequence voltage values are the same while generating either set of plots, and hence Figures 3.17 - 3.20 are simply scaled versions of Figures 4.1 - 4.4. Thus, although Figures 3.17 - 3.20 are more meaningful in determining thresholds, they do not hold any advantage as features for machine learning over Figures 4.1 - 4.4.

In this thesis, a multi-class Support Vector Machine classifier has been used to find the location of faults in the islanded distribution system.

4.1 Support Vector Machine

SVM(Support Vector Machine), which Vapnik introduced in 1990, is a popular machine learning algorithm due to its features like better data generalization performance, regularization for nonlinear datasets, high accuracy, theoretical guarantees regarding overfitting, and linearization of data with kernel [12]. SVM, which is used for high dimension datasets, has been proven accurate for a wide variety of datasets [12].

A SVM classifier's goal is to produce a model (based on the training data), which predicts test data's target values. SVM acts as a decision surface (a hyperplane) in the feature space and maps the data to a predetermined, high-dimensional space (higher than the input dimensions) via a kernel function.

SVM is inherently a binary classifier, but it can be used to classify multiple class problems. There are many ways to solve multi-class classification problems for SVM, such as Directed Acyclic Graph (DAG), Binary Tree (BT), One Against-One (OAO), and One-Against-All (OAA) classifiers. [13]. In this thesis, One Against All (also called One vs. All) SVM classifier has been implemented in Matlab on sequence voltages to perform fault location in an islanded IEEE 13-bus distribution system.

One vs. all trains the input data such that it compares every class with all other classes separately, as shown in Figure 4.5. OAA generates N-binary classifier models where N is the number of classes. In Figure 4.5, when class 1 is compared with all other classes (in this case, Class 2 and Class 3), Class 1 is considered as +1, and the rest is considered -1. The same procedure is applied for comparing Case 2 with the rest and Case 3 with the rest. Then all comparisons are added. The maximum of all the comparisons identifies which class is the testing input.

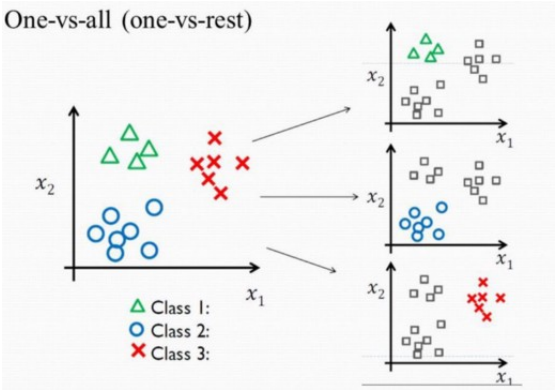

Figure 4.5: One vs All support vector machine method[14]

The following steps have been applied in using the OAA method:

1. Using fault analysis for four types of faults in the IEEE 13-bus distribution system, the sequence voltages at INV1 terminals are taken as input. The location of the fault is based on the fault distance in terms of number of feeder sections between the fault and INV1. SVM classifier should specify this distance based on the input data.

2. The input data has been balanced using the Up Sampling method to generate accurate models. Then the data have been split randomly into training and testing data. 70% of data have been used for training, and 30% of data have been used for testing.

3. RBF(Radial Base function) kernel has been proved to be accurate for a large variety of datasets; therefore, the RBF kernel has been used to transform the input data into a high dimensional space. The number of hyperparameters which influences the complexity of RBF model selection is less in the RBF kernel[15].

4. After training the model with the training data, the testing data has been used to find the SVM model's accuracy.

When using the SVM classifier to locate the faulted section, misclassification occurred most of the time. Depending on the random number chosen for splitting data in to training and testing data, the accuracy of classification was between 0-40%. Results underscore the initial observation made from visual inspection that the patterns of sequence voltages at the inverters in figures 4.1-4.4 did not show clear difference for faults at many different locations. Apparently, using SVM (or in all probability other machine learning tools) to identify the fault location just with the sequence voltages at the inverter terminals is not feasible.

The insistence on using voltages only at the inverter terminals for this exercise is because the attempt is to develop a *local* tool.

Chapter 5

Conclusion

This thesis proposes a unique approach of using the sequence voltages at the inverter terminals to detect and classify faults in an unbalanced islanded distribution feeder fed by 100% IBRs, creating the most restrictive topology for protection. It has been shown that the behavior of voltages during faults is different than the traditional behavior modeled by boundary conditions, due to the nonlinear and unconventional behavior of the IBRs in response to faults. This requires time-domain analysis to observe fault voltages at the inverter terminals. Such analysis is performed in PSCAD with detailed inverter models, and sequence voltage profiles are created to formulate threshold values for detection and classification of all types of faults. It is observed that sequence component based approach is superior to undervoltage based approach and successfully detects and classifies all faults. Even faults at remote locations, where undervoltage approach is unrelaible for detection, are detected by the proposed approach.

A machine learning based approach using SVM to approximately locate the faulted section simply from local sequence voltage measurements at the IBR terminals is explored. However, it was found that there is not enough discrimination in sequence

voltage signatures to perform this task.

The future work will focus on gathering more data and measurements across the distribution systems at critical locations and using *all* measurements together as an input vector to find the location of a fault in an islanded distribution system. Such an approach might detect discrimination in input for faults at different buses, which might help to find the faulted section. Communication will be required to get data from other buses, and hence, the approach will cease to be a local tool.

Appendix A

Appendix A: Multi Class Support Vector Machine Classifier Matlab Code Used to Find the Location of Faults

A.1 SVM Code for Finding the Location of Line to Ground Fault

```
%Finding the location fault of a line to ground fault
clc
clear all
close all
%Input data
Inv1_Sec_Negative_LGFault=[1.1215527578631;1.1505617447532;
```

```
7       0.268702129784430;1.2244402693349;
8       1.1215527717113;1.2451963708768;1.1848471119013;
9       1.0932150819753;1.0714442526352;1.045939430454;
10      1.1463583084027;1.0120999856792;1.0310716203223];
11  Inv1_Sec_Positive_LGFault=[1.5329011695985;1.5431529641095;
12      2.3424112818788;1.4229784282586;1.5329011786887;
13      1.3933127380184;1.4691872981731;1.5624948997336;
14      1.5887263019937;1.6382438733208;1.5399738707992;
15      1.6774928523485;1.6600768284113];
16  Inv1_Sec_Zero_LGFault=[0.16277216492612;0.17481848612869;
17      0.055477476141472;0.17969807127707;0.16277217060781;
18      0.18387133522428;0.17169667040647;0.15793303001556;
19      0.15283652182915;0.16643931779851;0.17422680850982;
20      0.16154561729586;0.14627320520131];
21  %Adding 1 to location of faults as it is not advised to work
        with zeros in
22  %the location
23  INV1_Distance=[3;3;3;1;2;0;2;4;3;3;2;4;4];
24  INV1_D=INV1_Distance+ones(size(INV1_Distance));
25  %Balacning Data
26  V1=[4,6];
27  Y=INV1_D;
28  X=[Inv1_Sec_Zero_LGFault,Inv1_Sec_Positive_LGFault,
        Inv1_Sec_Negative_LGFault];
29  Data=[X,Y];
30  for i=V1
31      ZZ=repmat(Data(i,:),4,1);
```

```
32      Data=[Data;ZZ];
33  end
34  V2=[5,8];
35  for i=V2
36      ZZ=repmat(Data(i,:),2,1);
37      Data=[Data;ZZ];
38  end
39  % split up dat into roughly 70% training and 15% test
40  [m,n] = size(Data) ;
41  P = 0.70 ;
42  idx = randperm(m)  ;
43  trainData = Data(idx(1:round(P*m)),:) ;
44  testData = Data(idx(round(P*m)+1:end),:) ;
45  d=3;
46  %%%%%%%%%%%%%%%%%%%%%%%%%%%%%%%%%%%%%%%%%%%%%%%%%%%%%%%%%%%%%%%%%%%%%%%
47  %Training
48  for i=1:d
49      xx(:,i)=trainData(:,i);
50  end
51  t_train=trainData(:,4);
52  t_train=t_train';
53
54  for i=1:d
55      xt(:,i)=testData(:,i);
56  end
57  y_test=testData(:,4);
58  X_train=xx;
```

```
59 y_train=t_train';
60 X_test=xt;
61
62 %Modeling SVM
63 y_train=cellstr(num2str(y_train));
64 classes=unique(y_train);
65 ms=length(classes);
66 SVMModel=cell(ms,1);
67 for j=1:numel(classes)
68     indx=strcmp(y_train,classes(j));
69     SVMModel{j}=fitcsvm(X_train,indx,'ClassNames',[false true
        ],'Standardize',true,...
70         'KernelFunction','rbf');
71 end
72 %Predicting the location for test data
73 classest=unique(y_test);
74 for j=1:numel(classest)
75     [~,score]=predict(SVMModel{j},X_test);
76     Scores(:,j)=score(:,2); % Second column contains positive
        -class scores
77 end
78
79 [~,maxScore]=max(Scores,[],2);
80 result=maxScore;
81
82 %%calculating the accuracy
83 accuracy = sum(y_test == result)/length(y_test);
```

```
84 accuracyPercentage = 100*accuracy;
85 fprintf('Accuracy = %f%%\n',accuracyPercentage)
```

A.2 SVM Code for Finding the Location of Double Line to Ground Fault

```
1 %Finding the location fault of a double line to ground fault
2 clc
3 clear all
4 close all
5 %Input data
6 Inv1_Sec_Negative_LLGFault
      =[0.53847828869171;0.38605560999372;
7       0.12868641741555;0.35550090048413;0.5384783078041;
8       0.28826232501211;0.40244294634377;0.53513315435068;
9       0.58708941440423;0.57560908697287;0.3877502709344];
10 Inv1_Sec_Positive_LLGFault
      =[0.665778144004;0.5280863292674;2.2501332557003;
11      0.40438171647409;0.66577820029776;0.32263020119523;
12      0.49688404170045;0.6919209046385;0.76030515440231;
13      0.76813221451105;0.52919818844766];
14 Inv1_Sec_Zero_LLGFault=[0.19843215906017;0.23145918186923;
15      0.040752191224217;0.26392878244482;0.19843217147767;
16      0.28661107792664;0.23801549455492;0.18904980993868;
17      0.1746174289663;0.20727864504476;0.23106942742242];
18 %Adding 1 to location of faults as it is not advised to work
      with zeros in
```

```
%the location
INV1_Distance=[3;3;3;1;2;0;2;4;3;3;2];
INV1_D=INV1_Distance+ones(size(INV1_Distance));
%Balacning Data
V1=[4,6,8];
Y=INV1_D;
X=[Inv1_Sec_Zero_LLGFault,Inv1_Sec_Positive_LLGFault,
    Inv1_Sec_Negative_LLGFault];
Data=[X,Y];
for i=V1
    ZZ=repmat(Data(i,:),4,1);
    Data=[Data;ZZ];
end
V2=[5];
for i=V2
    ZZ=repmat(Data(i,:),2,1);
    Data=[Data;ZZ];
end
% split up dat into rought 70% training and 15%
% test
[m,n] = size(Data) ;
P = 0.70 ;
idx = randperm(m)  ;
trainData = Data(idx(1:round(P*m)),:) ;
testData = Data(idx(round(P*m)+1:end),:) ;
d=3;
%%%%%%%%%%%%%%%%%%%%%%%%%%%%%%%%%%%%%%%%%%%%%%%%%%%%%%%%%%%%%%%%%%%%%%%%%%%%%%%
```

```
45 %Training
46 for i=1:d
47     xx(:,i)=trainData(:,i);
48 end
49 t_train=trainData(:,4);
50 t_train=t_train';
51
52 for i=1:d
53     xt(:,i)=testData(:,i);
54 end
55 y_test=testData(:,4);
56 X_train=xx;
57 y_train=t_train';
58 X_test=xt;
59
60 %Modeling SVM
61 y_train=cellstr(num2str(y_train));
62 classes=unique(y_train);
63 ms=length(classes);
64 SVMModel=cell(ms,1);
65 for j=1:numel(classes)
66     indx=strcmp(y_train,classes(j));
67     SVMModel{j}=fitcsvm(X_train,indx,'ClassNames',[false true
        ],'Standardize',true,...
68         'KernelFunction','rbf');
69 end
70 %Predicting the location for test data
```

```
71 classest=unique(y_test);
72 for j=1:numel(classest)
73     [~,score]=predict(SVMModel{j},X_test);
74     Scores(:,j)=score(:,2); % Second column contains positive
         -class scores
75 end
76
77 [~,maxScore]=max(Scores,[],2);
78 result=maxScore;
79
80 %%calculating the accuracy
81 accuracy = sum(y_test == result)/length(y_test);
82 accuracyPercentage = 100*accuracy;
83 fprintf('Accuracy = %f%%\n',accuracyPercentage)
```

A.3 SVM Code for Finding the Location of Three Phase to Ground Fault

```
1 %Finding the location fault of a three phase to ground fault
2 clc
3 clear all
4 close all
5 %Input data
6 Inv1_Sec_Negative_LLLGFault
    =[0.018017628327128;0.078963383097527;
7     0.003815496505184;0.018017593194096;0.001578156124246;
8     0.008641321256279;0.019679205368835;0.025911830441945];
```

```
Inv1_Sec_Positive_LLLGFault
    =[0.13971745965601;1.8078339995673;0.069108426750915;
     0.13971747789126;0.063397823450123;0.10440415661725;
     0.16927134767584;0.19260883522756];
Inv1_Sec_Zero_LLLGFault=[0.002216370777371;0.014548440533629;
     0.0006075506594;0.002216370863201;0.00025539072645;
     0.00053049043079;0.002044372571879;0.002745229041539];
%Adding 1 to location of faults as it is not advised to work
    with zeros in
%the location
INV1_Distance=[3;3;1;2;0;2;4;3];
INV1_D=INV1_Distance+ones(size(INV1_Distance));
%Balacning Data
V=[3,5,7];
Y=INV1_D;
X=[Inv1_Sec_Zero_LLLGFault,Inv1_Sec_Positive_LLLGFault,
    Inv1_Sec_Negative_LLLGFault];
Data=[X,Y];
for i=V
    ZZ=repmat(Data(i,:),2,1);
    Data=[Data;ZZ];
end
V2=[4];
for i=V2
    ZZ=repmat(Data(i,:),1,1);
    Data=[Data;ZZ];
end
```

```
Data=repmat(Data,1,1);
% split up dat into rought 70% training and 15%
% test
[m,n] = size(Data) ;
P = 0.70 ;
idx = randperm(m)  ;
trainData = Data(idx(1:round(P*m)),:) ;
testData = Data(idx(round(P*m)+1:end),:) ;
d=3;
%%%%%%%%%%%%%%%%%%%%%%%%%%%%%%%%%%%%%%%%%%%%%%%%%%%%%%%%%%%%%%%%%%%%%%%%%%%%%%%%
%Training
for i=1:d
    xx(:,i)=trainData(:,i);
end
t_train=trainData(:,4);
t_train=t_train';

for i=1:d
    xt(:,i)=testData(:,i);
end
y_test=testData(:,4);
X_train=xx;
y_train=t_train';
X_test=xt;

%Modeling SVM
y_train=cellstr(num2str(y_train));
```

```
60 classes=unique(y_train);
61 ms=length(classes);
62 SVMModel=cell(ms,1);
63 for j=1:numel(classes)
64     indx=strcmp(y_train,classes(j));
65     SVMModel{j}=fitcsvm(X_train,indx,'ClassNames',[false true
       ],'Standardize',true,...
66       'KernelFunction','rbf');
67 end
68 %Predicting the location for test data
69 classest=unique(y_test);
70 for j=1:numel(classest)
71     [~,score]=predict(SVMModel{j},X_test);
72     Scores(:,j)=score(:,2); % Second column contains positive
       -class scores
73 end
74
75 [~,maxScore]=max(Scores,[],2);
76 result=maxScore;
77
78 %%calculating the accuracy
79 accuracy = sum(y_test == result)/length(y_test);
80 accuracyPercentage = 100*accuracy;
81 fprintf('Accuracy = %f%%\n',accuracyPercentage)
```

A.4 SVM Code for Finding the Location of Line to Line Fault

```
%Finding the location fault of a three phase to ground fault
clc
clear all
close all
%Input data
Inv1_Sec_Negative_LLFault=[1.0210578839854;1.0606918168661;
    0.53478169847363;1.0504817075298;1.0210580511739;
    1.0533640409512;1.0358010611363;1.0084115657449;
    1.0051311910525;1.3508197197776;1.0495767869827];
Inv1_Sec_Positive_LLFault=[1.1208924005647;1.1836044229461;
    2.1270077740552;1.0894258122302;1.1208925636867;
    1.0843837481084;1.1134468480664;1.1374288445668;
    1.1409248434963;1.5008339234354;1.1736429130148];
Inv1_Sec_Zero_LLFault=[0.011930873518029;0.004851687813228;
    0.018382612966192;0.012690974892807;0.011930876277571;
    0.012792253600937;0.012835503234309;0.011934755771026;
    0.012183096424076;0.020144572785147;0.004873362395426];
%Adding 1 to location of faults as it is not advised to work
   with zeros in
%the location
INV1_Distance=[3;3;3;1;2;0;2;4;3;3;2];
INV1_D=INV1_Distance+ones(size(INV1_Distance));
%Balacning Data
V1=[4,6,8];
```

```
Y=INV1_D;
X=[Inv1_Sec_Zero_LLFault,Inv1_Sec_Positive_LLFault,
    Inv1_Sec_Negative_LLFault];
Data=[X,Y];
for i=V1
    ZZ=repmat(Data(i,:),4,1);
    Data=[Data;ZZ];
end
V2=[5];
for i=V2
    ZZ=repmat(Data(i,:),2,1);
    Data=[Data;ZZ];
end

% split up dat into rought 70% training and 15%
% test
[m,n] = size(Data) ;
P = 0.70 ;
idx = randperm(m)  ;
trainData = Data(idx(1:round(P*m)),:) ;
testData = Data(idx(round(P*m)+1:end),:) ;
d=3;
%%%%%%%%%%%%%%%%%%%%%%%%%%%%%%%%%%%%%%%%%%%%%%%
%Training
for i=1:d
    xx(:,i)=trainData(:,i);
end
```

```
t_train=trainData(:,4);
t_train=t_train';

for i=1:d
    xt(:,i)=testData(:,i);
end
y_test=testData(:,4);
X_train=xx;
y_train=t_train';
X_test=xt;

%Modeling SVM
y_train=cellstr(num2str(y_train));
classes=unique(y_train);
ms=length(classes);
SVMModel=cell(ms,1);
for j=1:numel(classes)
    indx=strcmp(y_train,classes(j));
    SVMModel{j}=fitcsvm(X_train,indx,'ClassNames',[false true
        ],'Standardize',true,...
         'KernelFunction','rbf');
end
%Predicting the location for test data
classest=unique(y_test);
for j=1:numel(classest)
    [~,score]=predict(SVMModel{j},X_test);
    Scores(:,j)=score(:,2); % Second column contains positive
```

```
        -class scores
end

[~,maxScore]=max(Scores,[],2);
result=maxScore;

%%calculating the accuracy
accuracy = sum(y_test == result)/length(y_test);
accuracyPercentage = 100*accuracy;
fprintf('Accuracy = %f%%\n',accuracyPercentage)
```

References:

[1] Richard Bowers. *Updated renewable portfolio standards will lead to more renewable electricity generation*. 2019 (accessed November 7, 2020). URL: https://www.eia.gov/todayinenergy/detail.php?id=38492.

[2] National Conference of State Legislatures. *State Renewable Portfolio Standards and Goals*. 2020 (accessed Novemeber 7, 2020). URL: http://www.ncsl.org/research/energy/renewable-portfolio-standards.aspx#sc.

[3] S Conti. "Protection issues and state of the art for microgrids with inverter-interfaced distributed generators". In: *2011 International Conference on Clean Electrical Power (ICCEP)*. IEEE. 2011, pp. 643–647.

[4] Sigifredo Gonzalez, Nicholas Gurule, Matthew J Reno, and Jay Johnson. "Fault current experimental results of photovoltaic inverters operating with grid-support functionality". In: *2018 IEEE 7th World Conference on Photovoltaic Energy Conversion (WCPEC)(A Joint Conference of 45th IEEE PVSC, 28th PVSEC & 34th EU PVSEC)*. IEEE. 2018, pp. 1406–1411.

[5] Sukumar Brahma, Nataraj Pragallapati, and Mukesh Nagpal. "Protection of islanded microgrid fed by inverters". In: *2018 IEEE Power & Energy Society General Meeting (PESGM)*. IEEE. 2018, pp. 1–5.

[6] Sukumar Brahma. "Protection of Distribution System Islands Fed by Inverter-Interfaced Sources". In: *2019 IEEE Milan PowerTech*. IEEE. 2019, pp. 1–6.

[7] Phani Harsha Gadde and Sukumar Brahma. "Realistic Microgrid Test Bed for Protection and Resiliency Studies". In: *2019 North American Power Symposium (NAPS)*. IEEE. 2019, pp. 1–6.

[8] Phani Harsha Gadde and Sukumar Brahma. "Comparison of PR controller and PI controller for Inverter control in an Unbalanced Microgrid". In: *2020 North American Power Symposium (NAPS)*. IEEE. 2020.

[9] Qing-Chang Zhong. "Robust droop controller for accurate proportional load sharing among inverters operated in parallel". In: *IEEE Transactions on Industrial Electronics* 60.4 (2011), pp. 1281–1290.

[10] Qing-Chang Zhong and Yu Zeng. "Universal droop control of inverters with different types of output impedance". In: *IEEE access* 4 (2016), pp. 702–712.

[11] Theodoros Alexopoulos, Milan Biswal, Sukumar M Brahma, and Mohamed El Khatib. "Detection of fault using local measurements at inverter interfaced distributed energy resources". In: *2017 IEEE Manchester PowerTech*. IEEE. 2017, pp. 1–6.

[12] J Suriya Prakash, K Annamalai Vignesh, C Ashok, and R Adithyan. "Multi class Support Vector Machines classifier for machine vision application". In: *2012 International Conference on Machine Vision and Image Processing (MVIP)*. IEEE. 2012, pp. 197–199.

[13] Fereshteh Falah Chamasemani and Yashwant Prasad Singh. "Multi-class support vector machine (SVM) classifiers–an application in hypothyroid detection and classification". In: *2011 Sixth International Conference on Bio-Inspired Computing: Theories and Applications*. IEEE. 2011, pp. 351–356.

[14] Mohammed Terry-Jack. *Tips and Tricks for Multi-Class Classification*. 2019 (accessed November 27, 2020). URL: `https://medium.com/@b.terryjack/tips-and-tricks-for-multi-class-classification-c184ae1c8ffc`.

[15] Chih-Wei Hsu, Chih-Chung Chang, and Chih-Jen Lin. *A practical guide to support vector classification. 2003*. 2003.